CLM-R113

United Kingdom Atomic Energy Authority
RESEARCH GROUP
Report

TRANSVERSE INJECTION OF PLASMA INTO A LINEAR, STELLARATOR-LIKE MAGNETIC FIELD

R G CHAMBERS

Culham Laboratory
Abingdon Berkshire

1971

Available from H. M. Stationery Office

C.18

PRICE 25p

U D C
621.039.647.026

CLM-R 113

TRANSVERSE INJECTION OF PLASMA INTO A LINEAR, STELLARATOR-LIKE MAGNETIC FIELD

by

R. G. CHAMBERS

A B S T R A C T

The plasma injector to be described is capable of injecting $\sim 8 \times 10^{16}$ ion-electron pairs into the separatrix of a linear, stellarator-like magnetic field (i.e. an axial magnetic field, plus the magnetic field from an $\ell=3$ helical winding.) A further $\sim 4 \times 10^{17}$ ion-electron pairs go to the vacuum walls and are lost, during the injection. The total energy of the injected plasma trapped in the separatrix is $\sim$ 5J, and the transverse ion temperature is in the range 100-300 eV, depending upon the magnitude of B_z.

The plasma enters the magnetic field by polarisation and E X B drift, in agreement with the results of workers studying other types of transverse injector. The speed at which the plasma enters the magnetic field is low ($\sim 3 \times 10^4$ m/sec.) A theory is described, which attempts to explain some of the plasma loss taking place during the injection. The use of metallic walls in the vacuum chamber reduces the amount of plasma trapped inside the separatrix, probably due to shorting of the polarization electric field before the plasma can reach the separatrix.

Results of other plasma flow and plasma energy measurements are also presented. A double Langmuir probe study of the injected plasma shows that the electron temperature has an upper limit of $\sim$ 20 eV. Measurements with an ion energy analyser show that the ions are moving with mean energy $\sim$ 50 eV along the magnetic field.

Finally, a prediction is made of the suitability of this sort of injector for filling a large toroidal stellarator.

U.K.A.E.A. Research Group,
Culham Laboratory,
Abingdon,
Berkshire.

September 1971.

SBN: 85311 002 6

CONTENTS

1. INTRODUCTION

In recent years there has been considerable interest in the filling of stellarators by injecting plasma across the magnetic field, into the separatrix of the stellarator[1-6]. Other containment devices also use cross-field injection of plasma, for example, the Toroidal Octupole[7], the linear Quadrupole[8], and the Magnetic Mirror[9].

Much work has also been done on the injection of plasma across uniform, parallel magnetic fields[10-15]. One conclusion of these experiments is that a low β plasma may travel across a magnetic field by electric polarization and $\underline{E} \times \underline{B}$ drift, provided the number density n is large enough so that the dielectric constant of the plasma is much greater than unity, i.e.

$$K = 1 + \frac{m_i n}{\epsilon_o B^2} \gg 1 , \qquad \ldots (1)$$

where m_i = mass of one ion of the plasma and B is the magnetic field. Under the above condition, an electric polarization field $\underline{E} = (- \underline{V} \times \underline{B})$ is set up, and the velocity at which the plasma moves across the magnetic field is given by:

$$\underline{v}_\perp = \frac{\underline{E} \times \underline{B}}{B^2} , \qquad \ldots (2)$$

where $\underline{v}$ is the velocity of bulk motion of the plasma, and $\underline{v}_\perp$ is the component of $\underline{v}$ perpendicular to $\underline{B}$.

Baker et al[9,10] showed that the plasma traversing the magnetic field may be halted by draining the polarization charge by current flow along magnetic field lines to a shorting conductor located some distance away along the magnetic field. Dory et al[7], studying a toroidal octupole, noted that depolarization of the transversely-moving plasma stream can take place, and the plasma be halted, by current flow along magnetic field lines which have been cut twice by the same plasma stream; that is to say, the polarization electric field can be drained, in certain magnetic field geometries, even without the use of a shorting plate.

Akulina et al[4,5] show that plasma may be trapped in the magnetic containment region of a toroidal stellarator if two Bostick guns are fired towards one another, across the magnetic field. Travelling in opposite directions across the magnetic field, the electric polarities of the two plasma blobs will be in opposite senses and will cancel one another upon collision, thus bringing both blobs to a halt. The same authors also noted that plasma from only one gun can also be trapped in a toroidal stellarator.

The experiments to be described in this paper are a continuation of the work on gas-fed injectors started at the same laboratory by Ashby[1,2]. The mechanical design of the present injector remains closely similar to the original gun described by Ashby, the main points of difference being:-

(i) The present gun has an enlarged plenum of volume 0.0355 cm^3, holding 10^{18} molecules when filled to atmospheric pressure (its normal operating condition).

(ii) The gun passes a higher current (500 amps at peak) for a longer time (800 μsec) than before.

(iii) The gun is now being tested in larger magnetic field (up to 0.9 tesla) than formerly.

(iv) The vacuum vessel in which the gun is being tested is of larger internal diameter (30 cm) than formerly, which facilitates certain types of measurement.

The present injector is capable of injecting $\sim 8 \times 10^{16}$ ion-electron pairs into the separatrix. A further $\sim 4 \times 10^{17}$ pairs are not trapped and find their way to the vacuum walls. These figures should be compared with the $\sim 6 \times 10^{15}$ pairs (trapped in the separatrix) produced by the original gun of references (1, 2, 6), or with the 6×10^{13} pairs produced by the titanium washer gun of reference (3). The guns described by Akulina et al[4,5] were apparently capable of delivering $\sim 10^{15}$ ion-electron pairs to the stellarator separatrix.

2. DESIGN OF THE APPARATUS

The main parameters of the magnetic field and of the vacuum tube are noted below :

Maximum B_z	0.9 tesla
Maximum I_ℓ	220 kA
Maximum $B_z I_\ell$ (Strength limitation)	10^5 tesla amps
ℓ-winding radius	0.205 metres
Pitch length of ℓ-winding	1.6 metres
Separatrix radius (to apex of trefoil), depending on ratio B_z/I_ℓ	0.05 - 0.14 metre
Length of vacuum tube	4 metres
Internal diameter of vacuum tube	0.29 metre
Material of vacuum tube	Porcelain

Fig.1 gives a general view of the apparatus. The B_z magnetic field was provided by a total of 18 magnetic field coils driven by a 3200 μF condenser bank, which could be charged to a maximum of 18 kV. The rise-time of the B_z was 9 msec, and the decay time (after operation of the crowbar ignitrons)

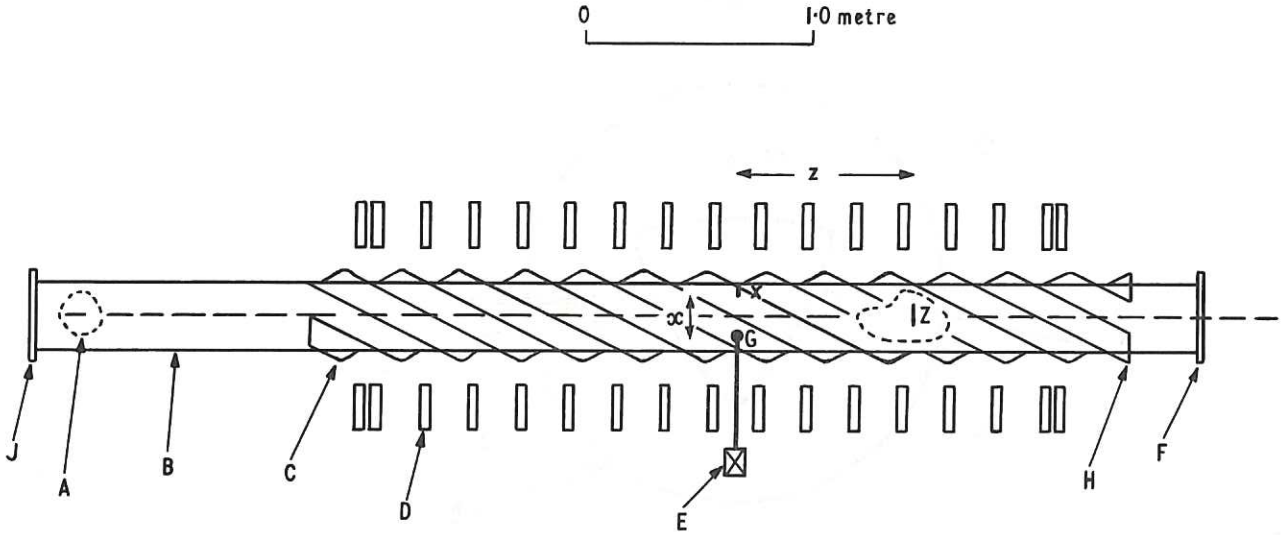

Fig.1 General view of apparatus.

A. 22.5 cm oil diffusion pump
B. vacuum tube
C. ℓ-windings, ℓ = 3, wound clockwise
D. B_z magnetic field coil
E. plasma gun
F,J. End plates
H. ℓ-winding current return

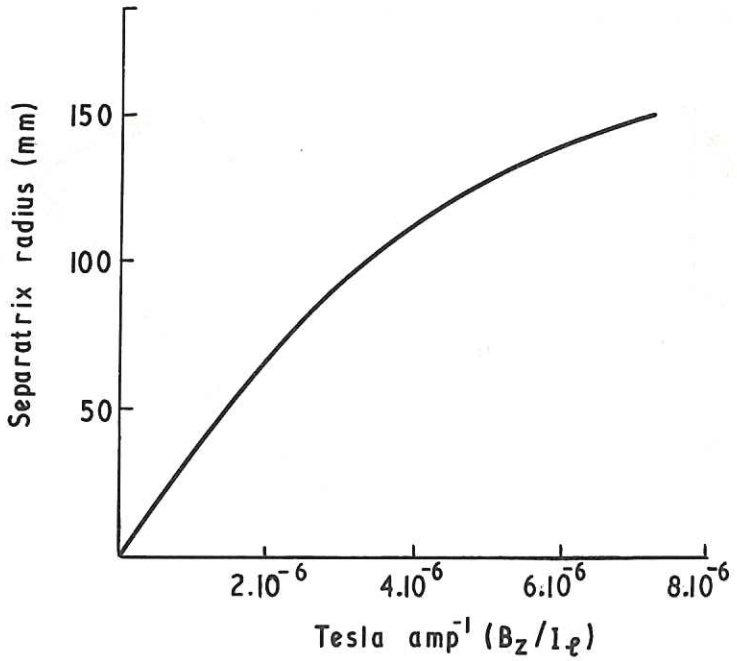

Fig.2 Computer program results for separatrix radius, plotted against $B_z/I\ell$.

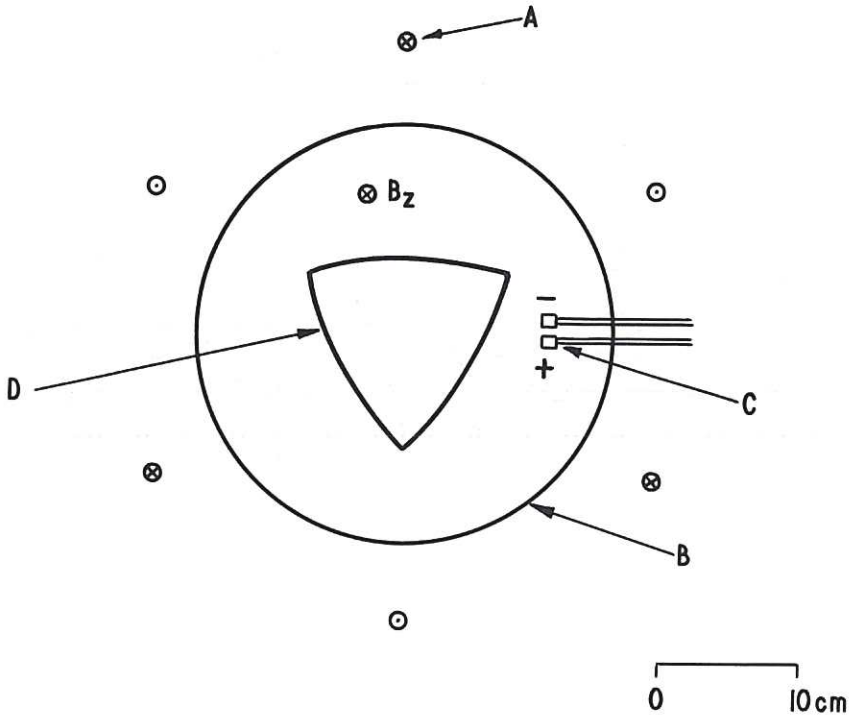

Fig.3 Relative dispositions of ℓ-windings (A) vacuum tube (B), plasma gun (C) and separatrix (D). The polarity of the gun and the direction of B_z is also shown.

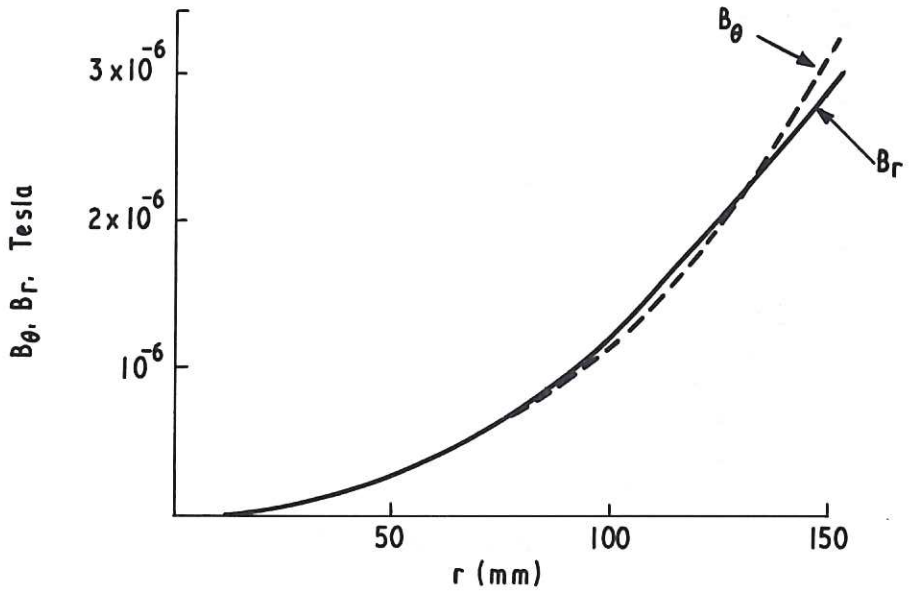

Fig.4 Maximum value of B_θ and of B_r, due to ℓ-winding current of 1 amp. Both are plotted against r.

was ~50 msec. The $\ell = 3$ helical windings were driven by a 21,000μF condenser bank, charged to a maximum of 7 kV. The rise-time of the ℓ-winding current was ~1msec, the decay time after crowbarring was ~10 msec. Electronic timing boxes ensured that both the B_z and the I_ℓ reached their maximum value simultaneously. The plasma injector was fired shortly after the time when the two banks were crowbarred, in the usual manner.

Fig. 2 plots computer program results for the separatrix radius (to the apex of the trefoil) as a function of B_z/I_ℓ. Fig.3 is a diagram of the directions of B_z and I_ℓ, and the relative dispositions of the separatrix and the plasma injector. The case of +ve I_ℓ is shown.

Fig. 4 plots $B_{r\ell}$ and $B_{\theta\ell}$ as functions r, when the ℓ-winding current $I_\ell = 1$ amp. $B_{r\ell}$ and $B_{\theta\ell}$ are respectively the maximum radial and azimuthal components of magnetic field for a given radial position r in the tube.

The vacuum tube was made from eight porcelain tubes, joined by rubber 'O' rings and evacuated to ~3×10^{-6} torr, by a 22.5 cm oil diffusion pump with a liquid nitrogen trap. The main components of the residual gas were H_2O(~70%), N_2 or CO(~25%) and O_2(~5%). Traces of atomic mass 2,40 and 44 were also present.

3. DESIGN OF THE PLASMA INJECTOR

Fig.5 is a diagram of the accelerator, which was powered by a 30μF condenser bank in series with a 1.4 mH inductance, a 10-Ohm resistance and an ignitron. The capacitor was normally charged to 9 kV. The discharge current produced by this LCR circuit was virtually independent of the impedance (~2 Ω) of the gun. The components of the LCR circuit were chosen so that the gun current would have the same shape and amplitude as the gas flow rate from the fast gas valve, i.e.,

$$I(t) = e\,\dot{N}(t),$$

where I is the gun current and $\dot{N}$ is the number of gas atoms flowing from the fast gas valve per second. This was one of the conditions tentatively assumed by Ashby[1] to be necessary for most efficient operation of the accelerator.

The accelerator works as follows:- The fast gas valve is actuated, which releases gas into the space between the gun electrodes. The gas is broken down by a 3 kV trigger pin in the cathode, and gun current flows between anode and cathode. This current, combined with the magnetic field of the trap, gives a force on the plasma towards the centre of the trap.

We now discuss the criteria that are necessary in order to maximize the amount of plasma energy produced by the gun. Many of the arguments presented belong to Ashby[14].

A transient heat pulse of energy $\mathcal{E}$ and duration t is dumped into the accelerator electrodes when the accelerator is fired. The condition for

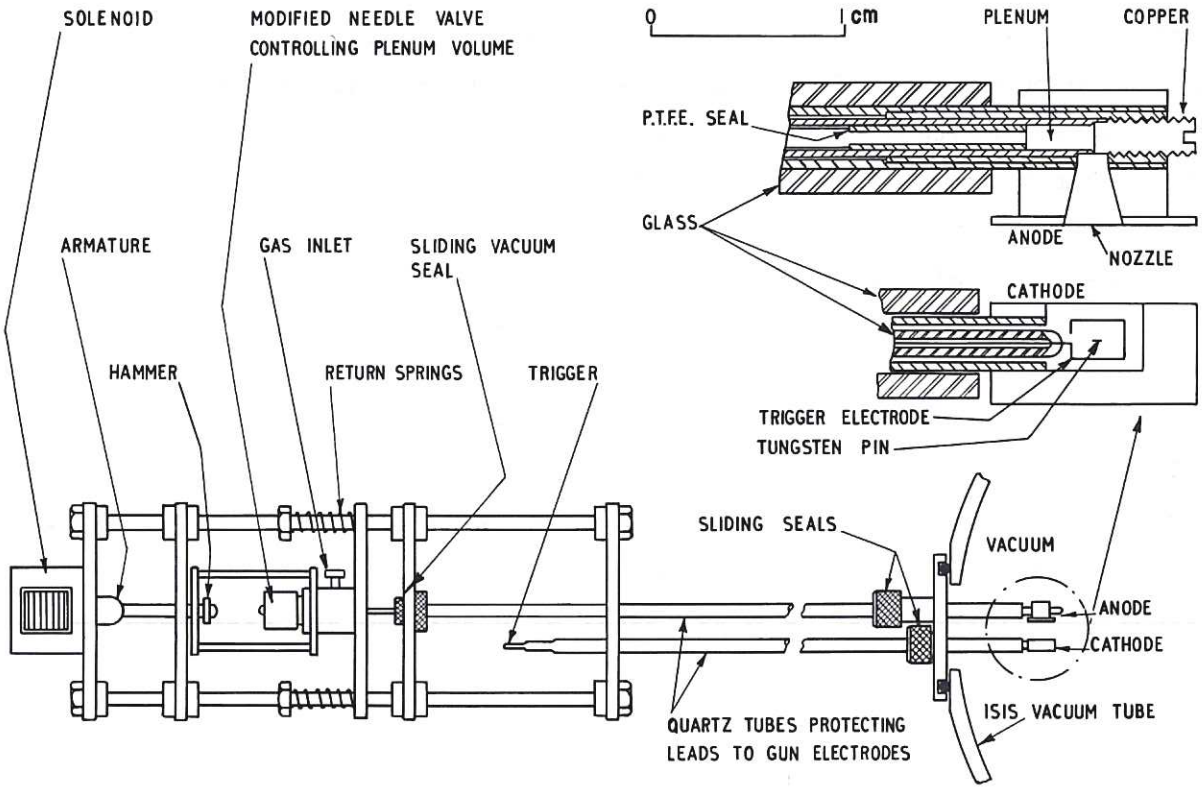

Fig.5 Diagram of the plasma gun.

this heat pulse not to cause melting of the electrode surfaces (with consequent introduction of impurity into the plasma) is:-

$$\mathcal{E} < \tfrac{1}{2}(T_M - T_A)\, A\, (\pi k \rho \sigma t)^{\frac{1}{2}} \qquad \ldots(3)$$

where the electrode material is normally at temperature T_A, has melting point T_M, thermal conductivity k, density ρ and specific heat σ. A is the area of cross-section of the discharge.

The electrodes can therefore be subject to higher energy pulses without surface melting if (i) the figure of merit, $(T_M - T_A)(\pi k \rho \sigma t)^{\frac{1}{2}}$, of the electrode material, is maximized; (ii) A is large; (iii) t is large.

For ease of manufacture, the electrodes of the present accelerator were copper, which has a figure of merit 55% of the maximum available (that of tungsten).

The area A of the discharge is limited to a small area ($\sim 1\ cm^2$) around the gas jet from the fast gas valve. This parameter cannot easily be changed by the experimenter.

The pulse time t of the injector must be kept much less than the plasma containment time of the toroidal stellarator which the present injector is designed to fill. It is found experimentally[3,6] that the containment time τ of plasma in a toroidal stellarator is about $10\,\tau_B$, where τ_B is the Bohm containment time.

We set:

$$t = 0.1\,\tau = \tau_B = \frac{2.8\,B\,r_p^2}{T_e}\,, \qquad \ldots (4)$$

where B is the magnetic field, and r_p the plasma radius, in the proposed stellarator. T_e eV is the electron temperature of the plasma produced by the guns. From equations (3) and (4), the maximum waste energy that may be dumped in each electrode without surface melting is given by:

$$\mathcal{E}_{max} = \tfrac{1}{2}(T_M - T_A)\,A\,(\pi\,k\,\rho\,\sigma)^{\frac{1}{2}}\left(\frac{2.8\,B\,r_p^2}{T_e}\right)^{\frac{1}{2}}. \qquad \ldots (5)$$

The present accelerator is intended eventually for injection purposes into a stellarator whose separatrix radius will be in the range 0.05 - 0.15 metres, and whose main B_φ magnetic field will be in the range 0 - 2 tesla. Arbitrarily selecting B = 1 tesla and r_p = 0.07 metres, and putting T_e = 20 eV, we find from equation (4) that the optimum duration of injection is about 700 μsec. Accordingly, the accelerator has been made with a gas flow and current pulse both ~700 μsec long.

4. EXPERIMENTS ON THE OPERATION OF THE ACCELERATOR

In all experiments, unless noted to the contrary, the fast gas valve plenum was filled with hydrogen to one atmosphere pressure (absolute). The rate of flow of hydrogen from the fast gas valve, upon operation, was measured with a fast ionization gauge[15], and the results are shown in Fig.6.

The current passed by the accelerator was measured by observing (via a high frequency filter) the voltage drop across an 8.55 mΩ resistance placed in series with the accelerator. The result, which was largely independent of gun impedance, is shown in Fig.7. Good matching has been achieved between the current and the gas flow, by suitable choice of circuit elements.

The voltage V that is maintained between the accelerator electrodes during the discharge was measured directly by means of a 180:1 voltage attenuator. This voltage measurement was done (a) as a function of the applied magnetic field B_z, (b) as a function of the spacing d between the accelerator electrodes, and (c) as a function of which gas (H_2, D_2, He, N_2 or A) was used to fill the fast gas valve plenum.

It was tentatively predicted in reference (1), that if the ions are the main current carriers between the accelerator electrodes,

$$V \sim \frac{e\,B^2\,d^2}{2m_i}\,. \qquad \ldots (6)$$

An oscilloscope trace of a voltage measurement, filtered to rid it of high frequency hash, is shown in Fig.7. Fig.8 plots V against B for hydrogen for various values of d.

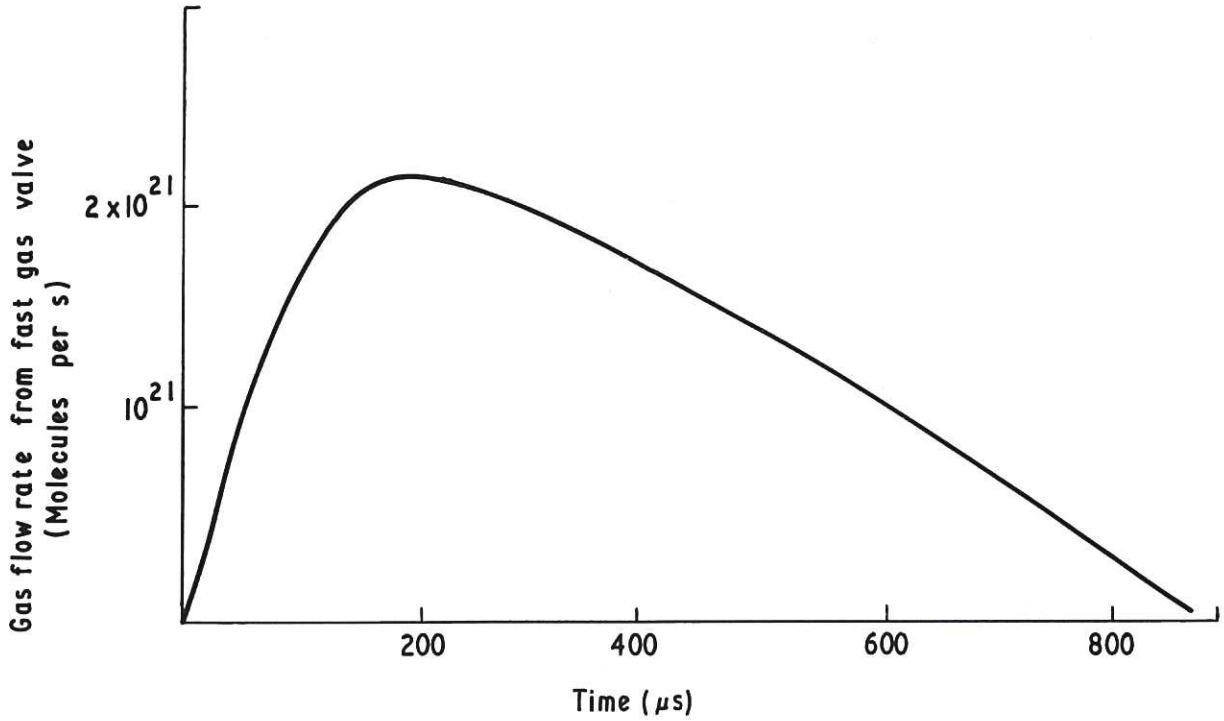

Fig.6 Gas flow rate from fast gas valve. Plenum pressure = 1 atmosphere. Results have an accuracy estimated to be ± 20%.

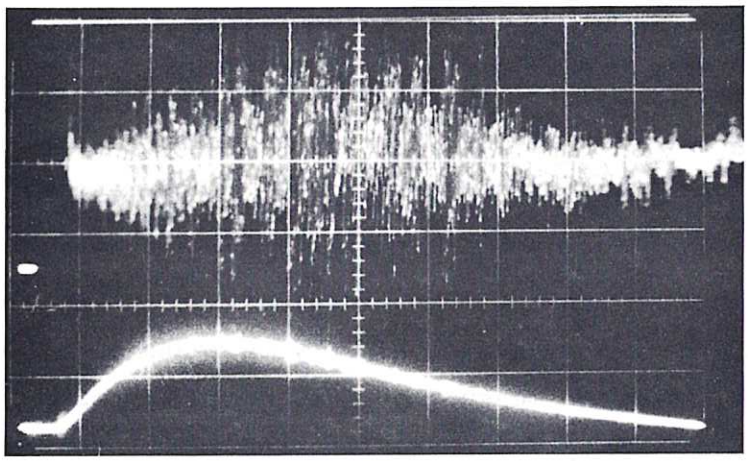

Fig.7 Upper beam: Voltage maintained between gun electrodes. 360 volts/large division, 100 μs/large division. Lower beam: current carried by gun. 580 Amps/large division, 100 μs/large division. B = 0.54 Tesla, d = 4.5 mm.

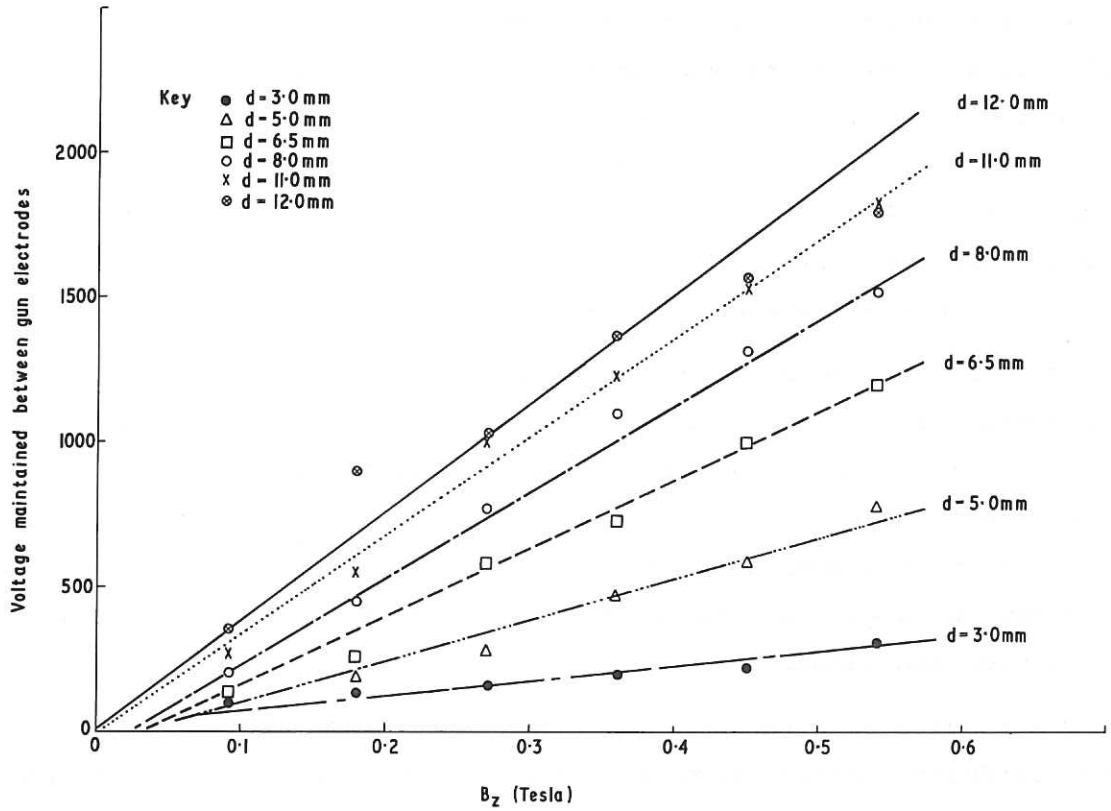

Fig.8 The voltage maintained between the gun electrodes plotted against B, for various separations d of the gun electrodes. Each point is the average of six observations. The estimated error bar is ± 30%.

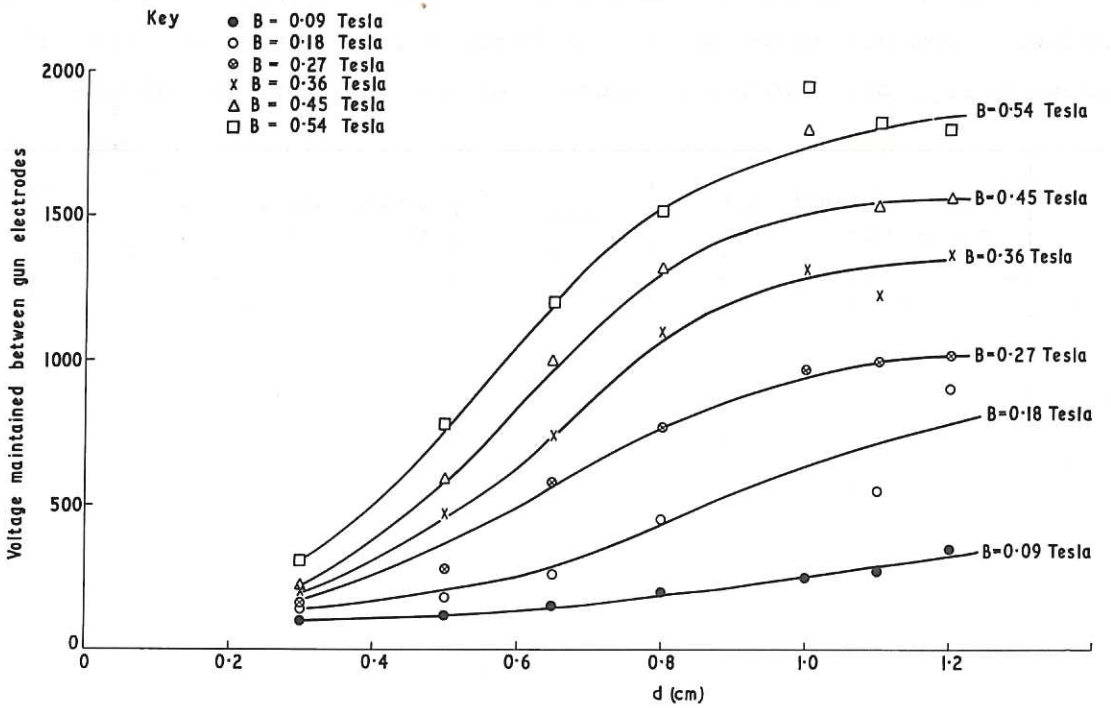

Fig.9 Voltage maintained between the gun electrodes, plotted against the gun electrode separation d, for various different values of B. Each point is the average of six observations, with an estimated error bar of ± 30%.

The law $V \propto B^2$ could possibly be fitted to the results in the range $B = 0 - 0.3$ tesla, which is the range studied by Ashby[1]. However, the (possible) square law breaks down beyond 3 kG. The best fit to the results in the whole of the range $0 - 0.8$ tesla studied by the present author, is:

$$V \propto B .$$

This result is similar to that of other authors working with electrical discharges in magnetic fields[16,17], and may be due to non-classical transport of electrons between the two electrodes.

For practical reasons, d could be varied only between 3 and 13 mm. With the spread of the results and the small range of d, it is not possible to get completely unambiguous results for the variation of V with d. However, the results of Fig.9 gives a better fit for $V \propto d$ than it would for $V \propto d^2$. This again supports the view that the voltage appearing between the electrode may be largely determined by non-classical transport of electrons between cathode and anode.

The results obtained when B and d were fixed, but m_i was varied (by using different gases), showed no general trend and V could not be described as being inversely proportional to m_i.

The heat dumped by the discharge onto the accelerator electrodes was measured with a small alumel-chromel thermocouple, and the results are tabulated below. From our knowledge of the total charge passed per shot (0.27 C), the average energy per impinging electron or ion can also be calculated.

B_z	Energy dumped in anode per shot	Average energy of impinging electron	Energy dumped in cathode per shot	Average energy of impinging ion
(tesla)	(Joules)	(eV)	(Joules)	(eV)
0.09	14.4	53	6.1	22
0.18	19.5	72	12.3	45
0.27	24.0	89	16.0	59
0.36	24.2	90	20.3	75
0.45	28.2	104	24.6	91
0.54	27.0	100	25.0	93

The energy of the ions impinging upon the cathode is approximately equal to the energy of the electrons impinging upon the anode. The structures of the anode and cathode sheaths are not known, so it is not possible to say whether the energies of the ions and electrons are the same in the whole of the space between the accelerator electrodes. The above table, however, may be taken as further (circumstantial) evidence of a substantial proportion of the accelerator current being carried non-classically by

electrons. The energy of the impinging ions and electrons on the electrodes is less than the measured voltage drop between the accelerator electrodes (c.f. Fig.8).

The weight loss of the electrodes per shot of the accelerator was measured by means of a chemical balance (capable of weighing to six significant figures). The measurement was obtained with $B_z = 0.36$ tesla, and is summarized in the table below.

Electrode	Weight lost per shot with B = 0.36 tesla	Number of atoms of copper lost per shot
	± 15%	± 15%
Anode	1.87×10^{-6} gm	1.75×10^{16}
Cathode	6.25×10^{-6} gm	5.85×10^{16}

These figures give a measurement of the extent to which the plasma is copper-polluted, and should be compared with the 2×10^{18} H atoms in the fast gas valve plenum, or the $\sim 5 \times 10^{17}$ ion electron pairs produced by the accelerator, or the $\sim 8 \times 10^{16}$ ion-electron pairs trapped in the separatrix when the gun is fired.

The weight loss is worse from the cathode than it is from the anode. Fig.10 is a photograph of the anode and cathode after several thousand shots. The cathode shows no sign of melting, but appears abraded; it has probably

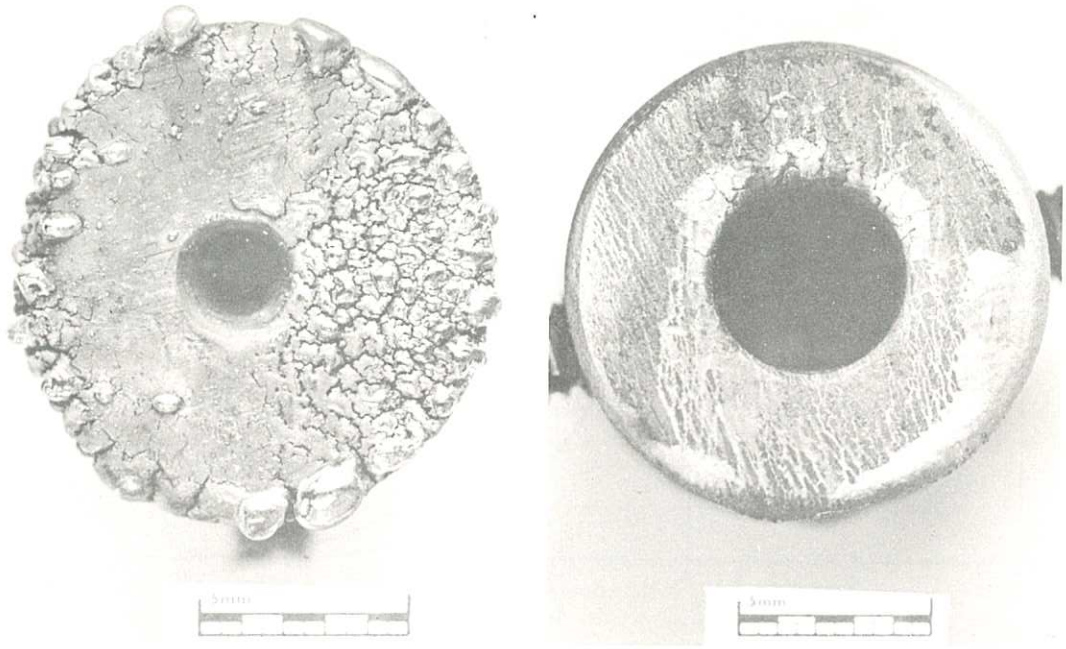

Fig.10 Anode (left) and cathode (right) after several thousand shots.

lost its weight by sputtering processes. The anode shows extensive signs of melting, probably the result of intense local arc-spot formation. It is believed that the gun is operating now at powers close to the maximum, and that further increase in gun power will lead to excessive electrode erosion.

5. OBSERVATIONS ON THE FLOW OF PLASMA ACROSS THE MAGNETIC FIELD

Using a B_z field alone (i.e. $I_\ell = 0$), the plasma electric field (transverse to B_z) was measured with an electric field probe. These measurements were based on the work of Baker et al[9,10], as described in the Introduction, and had the aims of determining:

(a) Whether the plasma produced by the present accelerator has an electric field in it that could explain the transverse drift of plasma from the gun into the separatrix (in the case of $I_\ell \neq 0$).

(b) The speed of this transverse plasma drift.

(c) How effectively the transverse plasma flow can be arrested by draining the electric polarization charge by current flow along magnetic field lines.

These measurements are relevant to the injection and trapping processes occurring when the gun is used to fill a stellarator.

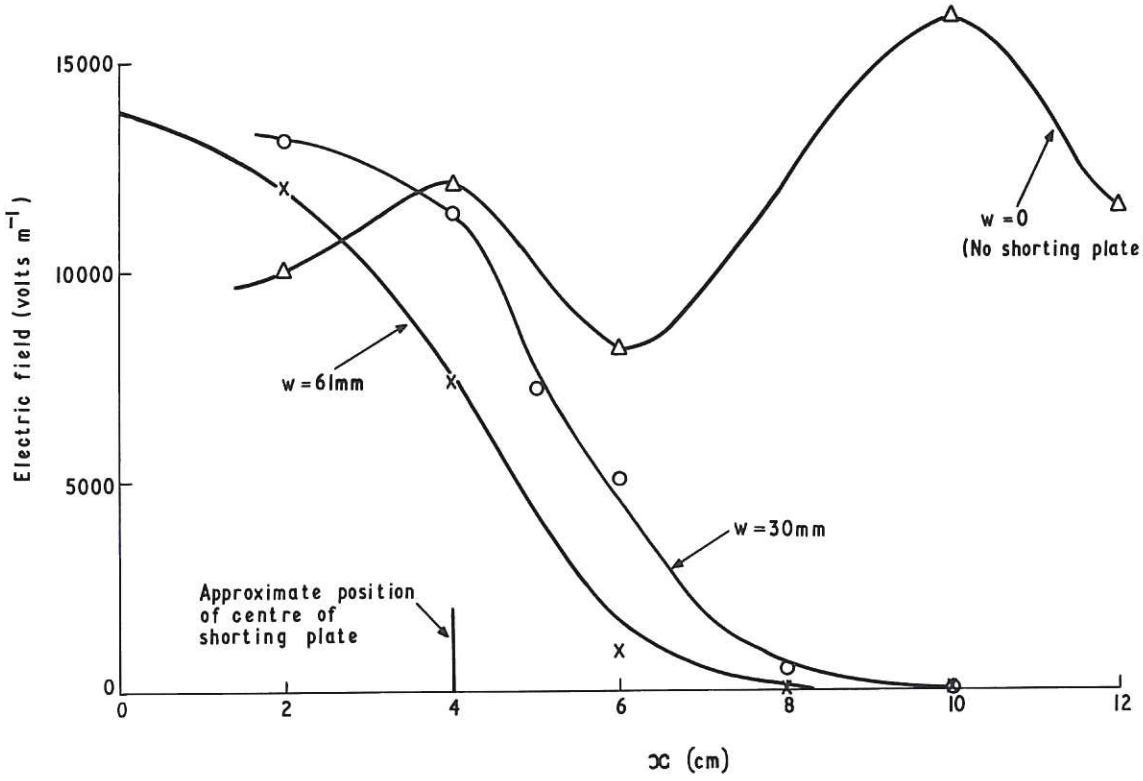

Fig.11 Electric field probe measurement, for different widths w of the shorting plate. Magnetic field B_z = 0.36 Tesla. Each point is the average of 6 observations, and has an error bar ± 15%.

Fig.1 shows a stainless steel strip of width w, placed in position Z (axial position Z = 92 cm from gun), diametrically across the vacuum tube. To prevent spurious depolarization of the plasma stream by the end plates, they were covered with insulator.

A high impedance electric probe[13,18,19], measuring $E_\perp$ (the electric field perpendicular to the plane G X Z), and having two electrodes of width 1.5 cm, length 2.0 cm, and separation 2.0 cm, was placed in position X at a distance x from the gun. The results quoted below are independent of the electric field probe's input resistance, which was varied between 66 kΩ and 660 kΩ.

Fig.11 shows the variation of $E_\perp$ with x, for different widths w of the shorting strip. Different magnetic fields produced similar results. $E_\perp$ is calculated directly from the voltage difference between the two probe electrodes, without correction for floating potential effects.

Without the shorting strip (W = 0) the electric field remains fairly constant across the tube. A shorting strip, even at axial distances Z = 92 cm, removes electric field from plasma attempting to cross the magnetic field lines linked to the shorting strip.

Time integrated photography showed, substantially, that the plasma failed to cross the magnetic field lines linked to the shorting plate (Fig.12).

An ion probe was stationed adjacent to the vacuum tube wall, opposite the injector, and without a shorting strip detected large plasma signals. These signals were greatly attenuated when shorting strips were introduced at position Z.

The plasma produced by our gun therefore moves across the magnetic field by polarization and $\underline{E} \times \underline{B}$ drift, and may be arrested by draining the polarization charge, similarly to the results of Baker et al[9,10].

The velocity of flow across the field lines is E/B[13]. This varies from 2×10^4 m/sec at B = 0.54 tesla, to 3.6×10^4 m/sec at B = 0.18 tesla.

Returning now to the study of injection into linear stellarators, the effect of having metallic vacuum tube walls was investigated by putting a non-magnetic stainless steel cylinder (internal diameter 28.5 cm, length 60 cm) into the vacuum tube. Its position relative to the gun was adjustable. Let s be the axial distance between the gun and the nearer-end of the cylinder. A large ion probe[1] recorded the signal from the trapped plasma in the separatrix. With $B_z = 0.36$ tesla and $I_\ell = 160$ kA, it was found that the large ion probe signal with s = 30 cm was $0.83\ S_o$, where

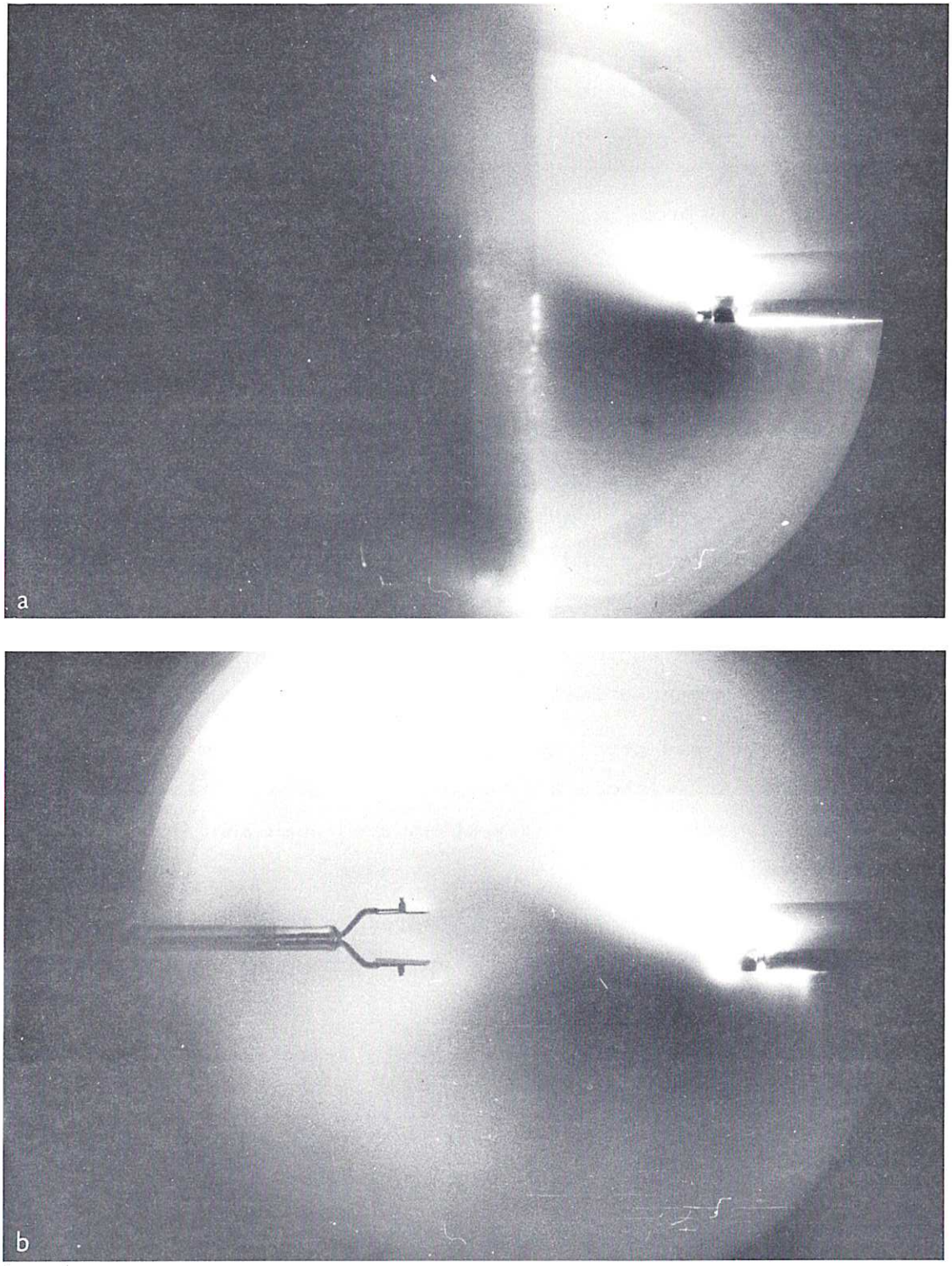

Fig.12 Time integrated photographs of plasma, (a) with a shorting plate 92 cm behind gun, (b) with no shorting plate. Also shown is the electric field probe.

S_o is the large ion probe signal with no stainless steel insert. When s was reduced to 15 cm, the large ion probe signal dropped to $0.46\ S_o$. Similar results were obtained with other values of B_z and I_ℓ. The centre of the gun electrodes was at a radial position $r = 9$ cm in the vacuum tube.

Consider magnetic field lines outside the separatrix of the stellarator. Fig.13 is a computer result, and plots the axial distance z that a magnetic field line extends before hitting a wall of radius 14.25 cm, having started at radial position r along a line joining the centre of the tube to the gun. The magnetic field in Fig.13 is $B_z = 0.36$ tesla, $I_\ell = 160$ kA.

Fig.13 shows that, if the stainless steel insert extends from $z = 15$ to $z = 75$ cm, its shorting effect is equivalent to that of a strip of width 2.1cm. For a metal insert extending from $z = 30$ to $z = 90$ cm, the shorting effect of the wall is equivalent to that of a shorting strip 0.75 cm wide. Plasma traversing a wide region of magnetic field lines linked to a metallic wall reaches the separatrix much attenuated. Injection by the present accelerator is possible only if the region of magnetic field, linked to metallic vacuum tube walls and interposed between the gun and the separatrix, is narrow.

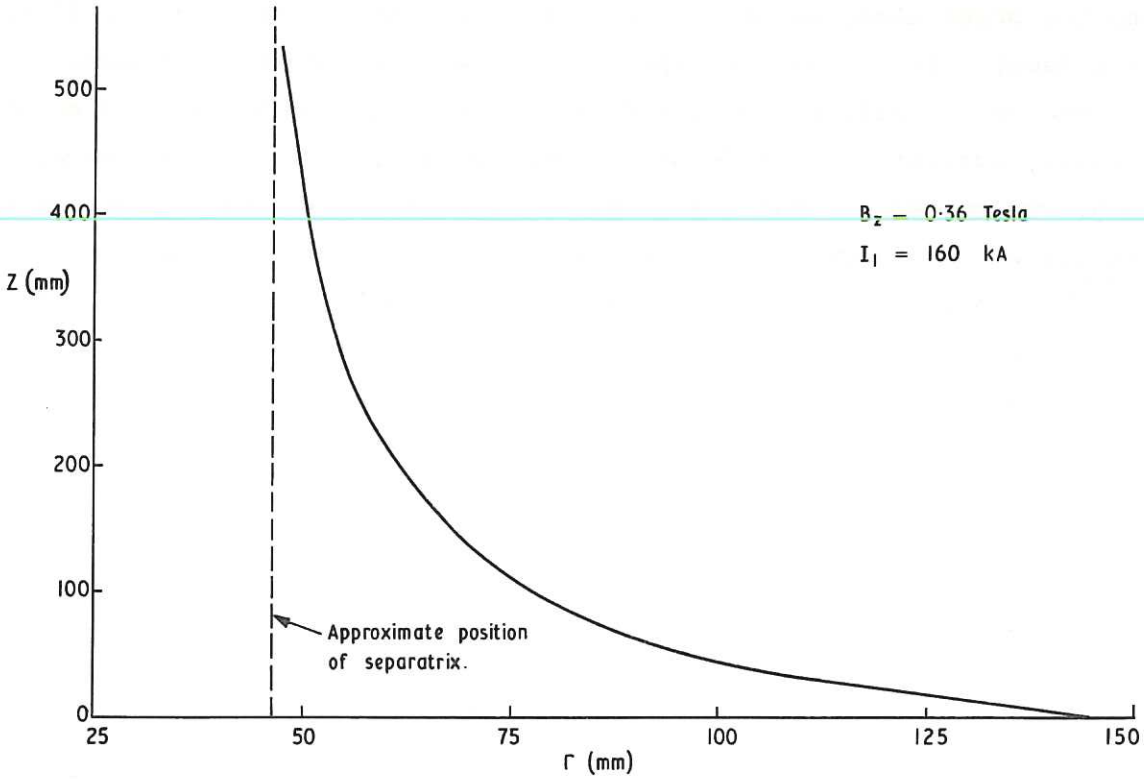

Fig.13 (Computer Result). The axial distance z that a magnetic field line extends before hitting a wall of radius 14.25 cm, having started at radial position r. (Refer to figure 15 for the definition of r).

6. OBSERVATIONS ON THE TRAPPING OF THE PLASMA IN THE SEPARATRIX

The existence of plasma trapped within a triangular separatrix was demonstrated as follows. A large ion probe[1] was constructed with two detectors. The inner detector was the size and shape of the separatrix obtained theoretically on a computer program. The outer detector of the large ion probe recorded all plasma coming to the probe outside the computed separatrix. With correct alignment of detector and separatrix the ratio of the outer inner detector signal was low. If the probe was rotated into misalignment, this ratio increased, because the outer detector was now recording some of the plasma inside the separatrix. This demonstrates the existence of plasma inside the computed separatrix.

The front face of the large ion probe is a stainless steel sieve material, which therefore shorts together all of the magnetic field lines coming to it inside the separatrix. The plasma stream from the injector is depolarized by the probe upon entering the separatrix, a condition necessary for the trapping of the plasma produced by the injector.

The efficiency of trapping of the plasma produced by the gun was measured as follows. A large ion probe measured the total amount of plasma reaching the probe along magnetic field lines inside the separatrix, (i.e. trapped plasma). In a separate experiment, the total amount of plasma reaching the vacuum wall was measured with a large ion probe, curved so as to fit snugly against the inside of the vacuum wall. This wall probe was 25 cm long, was curved so that its inner surface (the stainless steel seive) had a radius of curvature 12.5 cm centred on the axis of the tube, and spanned 90° of azimuth of the vacuum tube. The amount of escaping plasma was measured by scanning each quadrant of the tube, in turn, with the wall probe. In some measurements, while the wall probe was being used, a triangular piece of stainless steel was placed over the separatrix at an axial distance $z = 92$ cm from the gun. The triangular shorting plate was intended to depolarize and trap inside the separatrix the plasma from the accelerator, but was found to be unnecessary as the same results were obtained by the wall probe, with or without the triangle. Presumably without the triangle, the shorting takes place in the stainless steel end-plates of the vacuum tube.

Measured in the manner described, the trapping efficiency is tabulated below for $B_z = 0.36$ tesla, $I_\ell = 160$ kA, and for different values of the gap d between anode and cathode of the accelerator.

d mm	No. of ion-electron pairs going to wall	No. of ion-electron pairs trapped in separatrix	Trapping efficiency
3.5	10^{17}	8.0×10^{16}	45%
5.0	3.1×10^{17}	7.8×10^{16}	20%
7.0	2.8×10^{17}	4.9×10^{16}	15%
9.0	4.2×10^{17}	5.8×10^{16}	12%
13.0	5.0×10^{17}	6.0×10^{16}	11%

The errors of the measurements, due to an unexplained variation of the results from day to day, are as high as ± 25%. The number of ion electron pairs trapped in the separatrix was taken to be $1/e\alpha \int I\,dt$, where I is the current drawn by the large ion probe at time t, and α is the transparency of the front face (stainless steel sieve) of the large ion probe. The integration is performed over the whole of the injection pulse.

The plasma from the injector travels preferentially in one direction along the magnetic field, according to the polarity of the ℓ-winding currents. From Fig.3 it can be seen that at the gun there is a radial component $B_{r\ell}$ of magnetic field due to the ℓ-windings. $B_{r\ell}$ and the gun current give a component of force on the plasma into the paper in Fig.3. When the ℓ-winding currents are reversed, this component of the force on the plasma will be out of the paper. A large ion probe stationed at an axial distance $Z = 92$ cm from the gun recorded 5.8×10^{16} ions reaching it when $B = 0.36$ tesla and $I_\ell = +160$ kA. When $B = 0.36$ tesla and $I_\ell = -160$ kA, the number of ions reaching the probe was 2.8×10^{16} ions.

The results of the above table show an increase of trapping efficiency as the gap d is decreased. However, there is no corresponding increase in the total amount of plasma contained in the separatrix because of a decrease in the efficiency with which the gun converts the plenum gas into plasma. There are 2×10^{18} H atoms in the plenum. The efficiency of plasma production from the available gas is therefore 9% when $d = 0.35$ cm, and 28% when $d = 1.3$ cm. The waste gas probably appears as neutral gas in the plasma. Further measurements are obviously needed to determine directly the neutral density in the vicinity of the gun.

The mechanism by which the plasma escapes from the separatrix (or fails to be trapped by the separatrix) was studied as follows. A wall probe was screened so that only a narrow strip 2 cm wide could record plasma. This strip ran at an angle across the curved front face of the probe, and if extended would have the same axial period as the ℓ-windings (1.6 metres). This screened probe scanned along the lower quadrant of the tube. The signal

recorded by the screened probe, as a function of the axial distance Z, is plotted in Fig.14. B_z was 0.36 tesla and I_ℓ was 160 kA.

There are peaks at Z = 6, 46, and 60 cm. Fig.15 is the result of a computer program which followed magnetic field lines outside the separatrix. In following a field line, the axial position Z will change. A rotational correction is applied by the computer program so that the separatrix remains in the same orientation, i.e. we are following field-lines in a rotated space. Then, in Fig.15, lines such as ABC are the escaping field lines in the direction of B_z. Lines such as ADE are the escaping field lines in a direction opposed to B_z. By noting that the periodicity of the ℓ-winding is 160 cm, and comparing Figs.14 and 15, one sees that the screened probe peaks that occur at Z = 6 and Z = 60 are due to plasma escaping along field lines towards the gun. The peak at Z = 46 cm is due to plasma escaping along field lines away from the gun.

The fact that some plasma is escaping the 'wrong way' is probably the result of some plasma particles being localized, as described by Gibson et al[20]. It will be shown later that the plasma produced by the accelerator has a larger ion temperature transverse to the magnetic field than it has along the magnetic field, a condition which produces a large fraction of localized particles.

It would have been interesting to have inserted a small ion probe[1] inside the separatrix in the region within one field period of the gun, and to have observed the amount of plasma moving along field lines towards and away from the gun. Unfortunately, this was not possible because of the absence of probe entry ports within one field period of the gun port.

However, a small Faraday cup[1] was placed at an axial distance Z = 80 cm from the gun, through an entrance port. Fig.16 shows the plasma signal received by the probe, when the entrance hole of the probe was pointing along the magnetic field, (a) towards the gun, and (b) away from the gun. The magnetic fields in this experiment were B_z = 0.36 tesla, I_ℓ = 160 kA. The plasma moving towards the gun has about 20% of the intensity, on average, of the plasma moving away from the gun, possibly the result of localized particles in the plasma. With a linear stellarator, however, it is possible that some of this reverse plasma could be reflected from the end-plates. The results must therefore be treated with caution.

The escape mechanism of the plasma was further studied with a Faraday cup, this time near the vacuum tube wall, with its acceptance hole pointing towards the vacuum tube axis. The object of the experiment was to measure the relative amounts of plasma escaping along escape paths ABC,

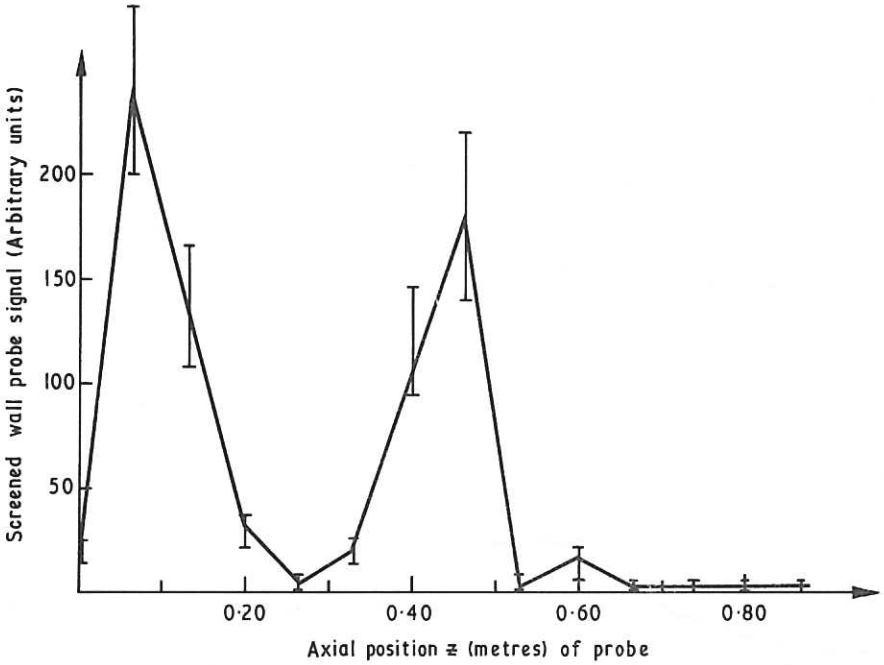

Screened wall probe signal, versus the axial position z of the probe relative to the gun. The probe is in the lower quadrant of the vacuum tube.

Fig.14 Signal recorded by the screened wall probe, showing maxima at z = 0.06, 0.46 and 0.60 metres.

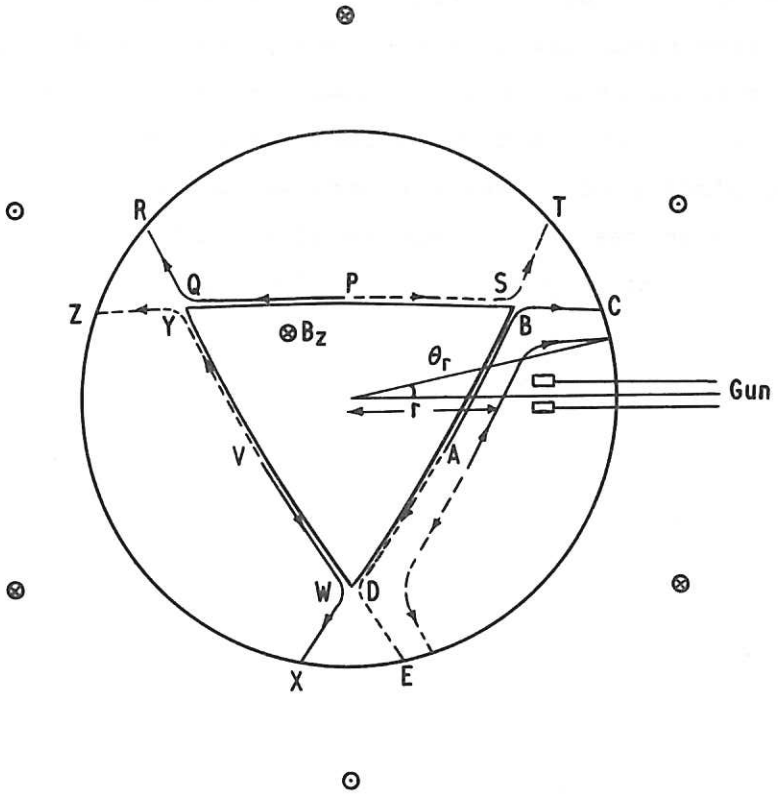

Fig.15 Diagram showing the plasma escape routes (in rotated space). (Computer result). The paths ABC, PQR and VWX are for plasma escaping parallel to B. The paths ADE, PST, VYZ are for plasma escaping antiparallel to B. The diagram also defines r and θ_r.

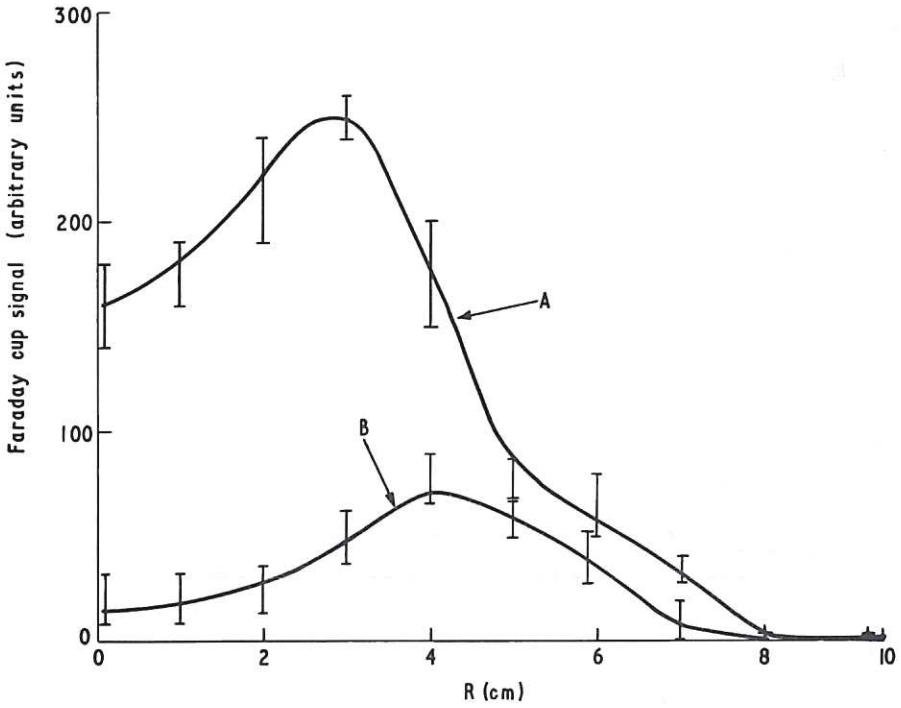

Fig.16 Faraday cup measurement, plotted against radial position r of the probe. Curve (A): Faraday cup acceptance hole pointing axially towards gun. Curve (B): pointing away from gun.

PQR and VWX in the rotated space of Fig.15. This measurement, and the measurement of the fine structure of the escape peaks, yields information on the plasma escape mechanism. Fig.17 shows the signal recorded by the Faraday cup at r = 120 mm, in the three tridrants* of rotated space. A triangular shorting plate placed over the separatrix (at Z = 0.80 metre) was used when obtaining these results, in the usual manner. The graphs were obtained by altering the axial position Z ($0.30 \leq Z \leq 0.55$ metres) of the probe, which was in a constant azimuthal position in real space. This is equivalent to altering the azimuthal position of the probe in rotated space. It is seen that:

(i) The escape of plasma is greater from the gun tridrant than from either of the other two tridrants.

(ii) The escape peak in the gun tridrant is wider than the other two peaks.

(iii) There is a double peak in the gun tridrant.

A substantial fraction of the escaping plasma is in the gun tridrant, probably plasma that has failed to reach the separatrix. The escape of plasma which has previously reached the separatrix, is evidenced by the escape peaks in the other two tridrants, and is almost as important.

---

*A tridrant is defined as a 120° sector of a circle

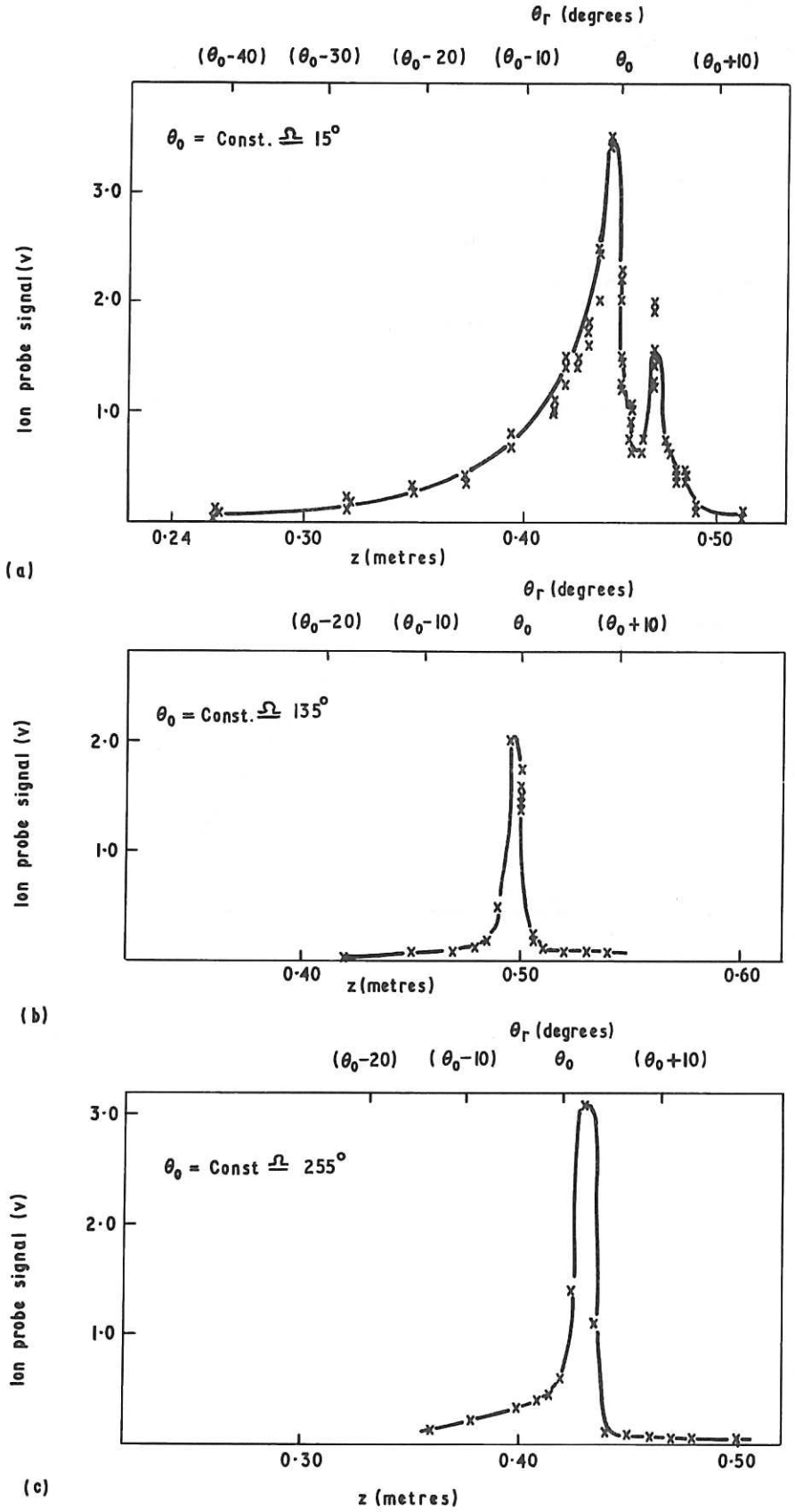

Fig.17 Results obtained with a Faraday cup placed near the vacuum tube wall, at radial position r = 120 mm. (a) with the probe studying escape peak ABC (refer to figure 15). Each point represents a measurement. (b) Escape peak PQR. At z = 0.50 metres, each point represents a measurement. Otherwise, each point is the average of three readings. (c) Escape peak VWX. Each point is the average of three readings.

The azimuthal position θ_r of the probe in rotated space is related to the azimuthal position θ_o in real space, to the axial position Z, and to the ℓ-winding period L by:

$$\theta_r = \theta_o + \frac{2\pi Z}{L} \quad .$$

It was not possible to measure θ_o with sufficient accuracy to be useful, although its value was kept constant for each case in Fig.17.

Fig.18 is a plot of θ_r against r (see Fig.15), obtained from a computer program which follows escaping magnetic field lines. Here $B_Z = 0.4$ tesla, $I_\ell = 160$ kA. Fig.18 indicates that the wide peak in the gun tridrant is the result of plasma particles starting at a wide range of radial positions outside the separatrix. The escape peaks in the other two tridrants are no wider than that which can be explained by Larmor radius effects.

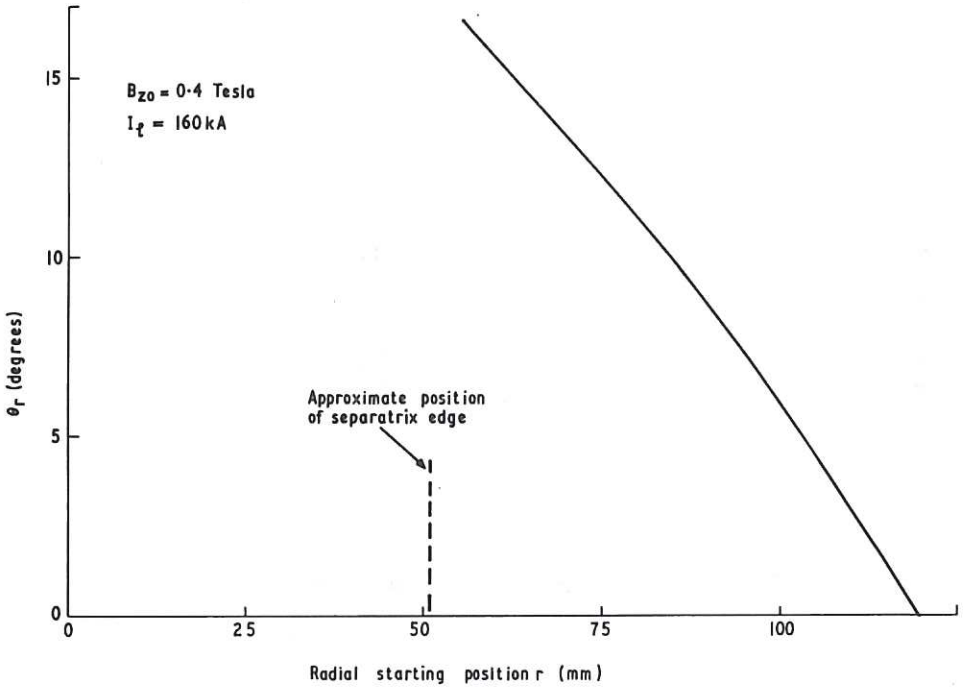

Fig.18 A plot of θ_r against r (computer result). Refer to figure 15 for definitions of θ_r and r. θ_r is measured to the point at which the radial position = 120 mm.

A theory is presented below, which explains with partial success the observations on plasma escape in the gun tridrant. Suppose the gun produces a plasma whose ions have a thermal velocity $v_{\|}$ along the local magnetic field, and that the plasma has an E × B drift velocity v_D perpendicular to the local magnetic field. The gun is located in a magnetic field where $B_\theta = 0$ and $B_r \sim \xi I_\ell r^2$. In our case, $\xi = 1.2 \times 10^{-4}$ (see Fig.4).

After time dt the position of the particle in rotated space will be changed by an amount:

$$dr = + (v_{\parallel} \sin\beta - v_D \cos\beta)\, dt$$

$$d\theta = + \frac{2\pi (v_D \sin\beta + v_{\parallel} \cos\beta)\, dt}{L}$$

$$dz = + (v_D \sin\beta + v_{\parallel} \cos\beta)\, dt$$

where

$$\tan\beta = \frac{B_r}{B_z} = \frac{\xi \cdot I_\ell\, r^2}{B_{zo}} \quad .$$

At the position of the gun, the side of the separatrix makes an angle $\pi/3$ radians with the radius vector. For the ion to move away from the separatrix and escape, the following criterion is necessary:

$$dr > r \cdot d\theta \cdot \cot(\pi/3) \, .$$

The condition for escape reduces to

$$v_{\parallel} \left[\xi\, I_\ell\, r^2 - \frac{2\pi r B_{zo}}{L\sqrt{3}} \right] > v_D \left[\frac{2\pi r^3 \xi\, I_\ell}{L\sqrt{3}} + B_{zo} \right] \, . \qquad \ldots (7)$$

The plasma escapes, according to the theory, because $v_{\parallel}$ along the outwards-sloping magnetic field line carries the ion away from the separatrix faster than v_D carries the ion towards the separatrix. When $v_{\parallel}$ is negative, this escape mechanism is in-operative. Fig.22 shows that the energy $E_{\parallel}$ of the plasma trapped in the separatrix is greater in one direction than the other, as predicted by the theory. The theory also explains the width of the escape peak in the gun tridrant. Ions with a large value of $v_{\parallel}/v_D$ will be lost at a greater effective starting radius r than those with a small value of $v_{\parallel}/v_D$. However, the theory is not so successful at explaining the results of Fig.21, which show that the amount of plasma trapped in the separatrix is only marginally dependent on the distance of the gun from the separatrix edge. The theory would have predicted a strong relationship between these two variables.

Inserting $r = 0.10$ metres, $B_r = 1.2 \times 10^{-4}\, I_\ell\, r^2$ into equation (7), and putting $B_z = 0.36$ tesla, $I_\ell = 160$ kA, the following condition for escape is obtained:

$$v_{\parallel} = \geq 3.6\, v_D \quad ,$$

which is satisfied by our plasma ($v_{\parallel} = 10^5$ m/sec, $v_D = 2.5 \times 10^4$ m/sec). At larger r, escape is even more easy. At smaller r, the escape theoretically becomes <u>rapidly</u> more difficult.

The gun position for the results of Fig. 17 was at $r = 0.095$ metres which means that part of the gun electrode was at $r = 0.10$ metres.

It is possible that, with $I_\ell \neq 0$, a wall shorting effect of the type recorded by Baker et al[9,10] may reduce v_D below the value measured when $I_\ell = 0$. This would make escape more easy.

7. ATTEMPTS AT INCREASING THE AMOUNT OF PLASMA TRAPPED IN THE SEPARATRIX

Experiments were performed, in which every available parameter which might affect the gun operation or trapping mechanism was altered in turn. Most of the results were negative or marginal. The only parameter tested that will substantially alter the amount of plasma trapped inside the separatrix is alteration of the gun current.

A large ion probe was placed at a distance $z = 92$ cm from the gun, and its signal was measured as the various parameters were changed.

(i) Alteration of B_z leaving B_z/I_ℓ constant

B_z/I_ℓ was kept constant in these experiments in order to eliminate any possible effect of a change of separatrix size, an effect that was tested separately. Fig.19 shows the large ion probe signal as a function of B_z for different B_z/I_ℓ. Within the range of B_z that could be studied because of the ℓ-winding strength limitation, no more than marginal changes are discernible.

(ii) Alteration of I_ℓ, keeping B_z constant

Again, no clear trend in the results is apparent. (See Fig.20).

(iii) Alteration of the gap d between anode and cathode of gun

The results of this experiment have already been described. Although plasma trapping efficiency improves if d is small, there is simultaneously less plasma output from the gun. The overall result is no marked improvement of the amount of plasma trapped in the separatrix when d is altered.

(iv) Variation of the distance of the gun from the edge of the separatrix

The gun was moved into various radial positions, keeping $B_z = 0.36$ tesla, $I_\ell = 160$ kA. Fig.21 shows that the plasma signal recorded by the large ion probe is virtually independent of the position of the gun relative to the separatrix if the gun remains outside the separatrix, (a condition necessary for the gun to be useful). The one exception to this result is when the gun is close to the vacuum wall, probably because of some wall-effect.

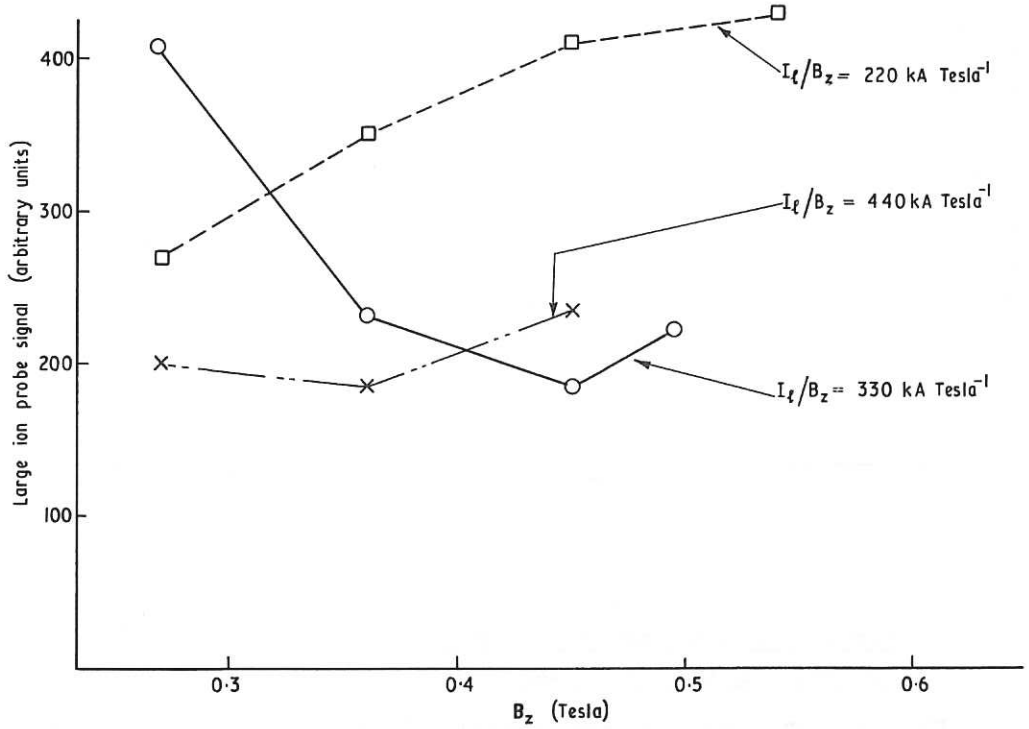

Fig.19 Large ion probe signal, plotted against B_z for various values of I_ℓ/B_z.

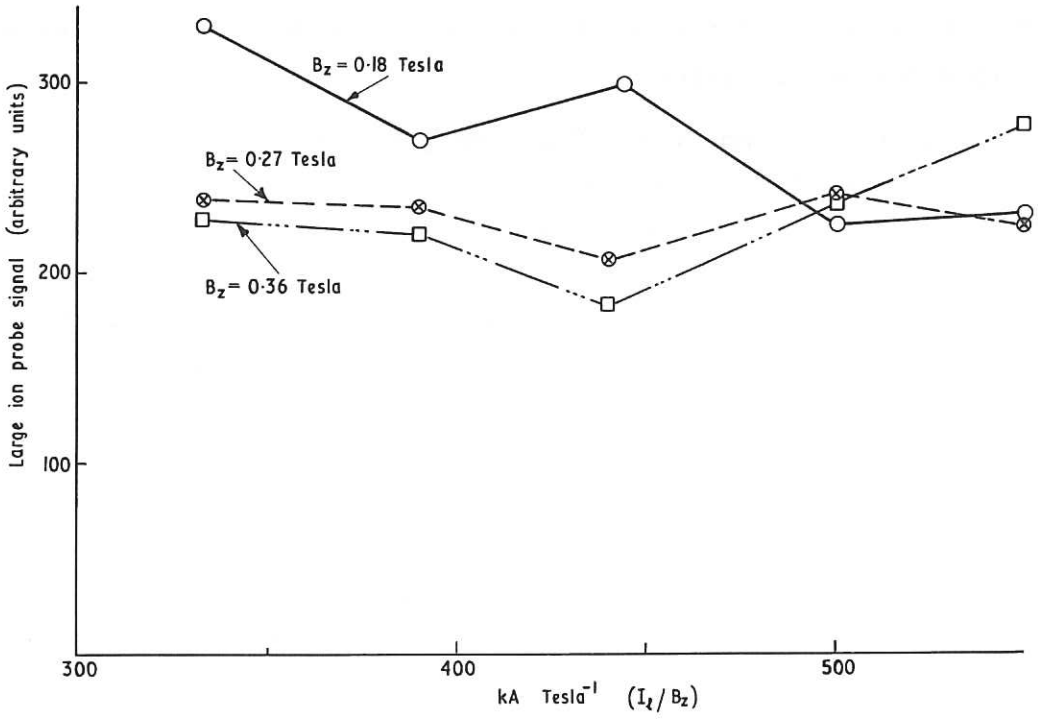

Fig.20 Large ion probe signal, versus (I_ℓ/B_z), for various values of B_z.

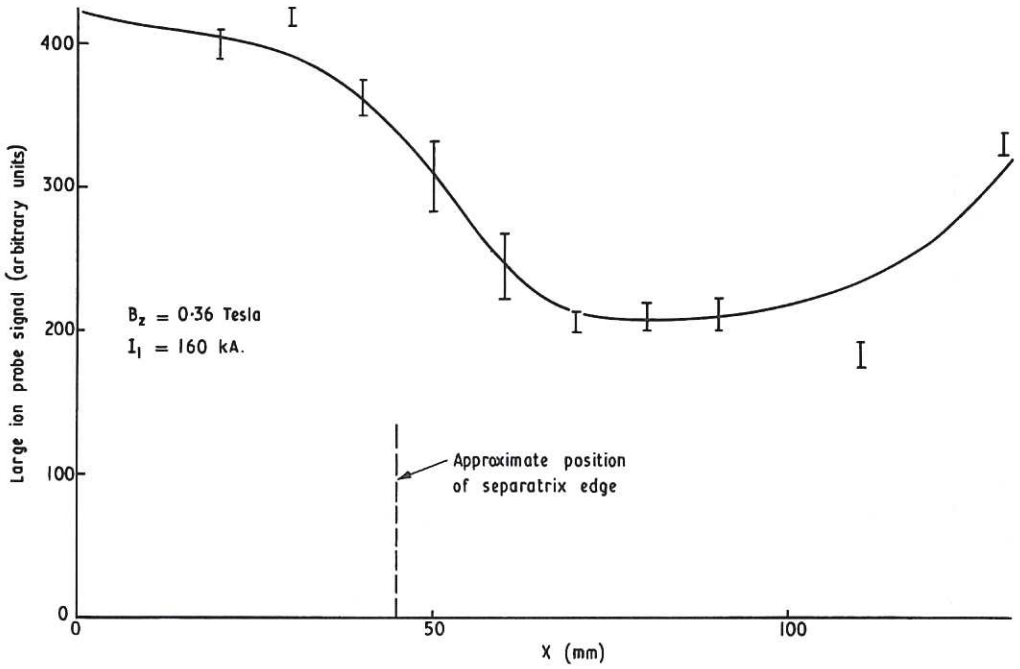

Fig.21 Large ion probe signal, versus radial position x of centre of gun electrodes.

(v) Variation of the amount of gas in the plenum of the fast gas valve

The plenum pressure was altered from 0.2 atmosphere (the minimum at which breakdown between the gun electrodes was possible) to 1 atmosphere. With this variation of plenum pressure, the amount of plasma recorded by the large ion probe remained constant, within experimental errors.

(vi) Firing two oppositely-directed guns towards one another into the separatrix

The experiment of Akulina et al[4,5], already summarized in the Introduction, was repeated with two of our guns. We obtained completely opposite results. Two of our guns fired towards one another into the separatrix of our linear stellarator, produced less trapped plasma in the separatrix than either gun alone. This may be due to either of the following differences between the two experiments:

(a) The present experiments were performed in a linear stellarator, with the probe also acting as a shorting plate. The experiments of Akulina were performed in a toroidal stellarator, with no shorting plates.

(b) Our gun produces plasma for a much longer time (~800 μs) than that of Akulina (~ 0.5 μs).

(vii) Alteration of the cross-sectional area of the gun electrodes

In view of the poor conversion efficiency of the plenum hydrogen into plasma, a new set of electrodes having four times the cross-sectional area of the original ones, was tested. The original (standard) electrodes had a diameter of 1.25 cm, and the new ones 2.5 cm. The table below charts the large ion probe signal (arbitrary units) for the two electrodes, under different values of B_z and I_ℓ.

B_z (tesla)	I_ℓ (kA)	Ion Probe Signal (1.25 cm electrodes)	Ion Probe Signal (2.5 cm electrodes)
0.36	160	4.5	5.6
0.36	200	4.1	5.7
0.36	120	5.7	6.2
0.36	80	11.0	7.2
0.45	200	4.5	5.1
0.45	150	5.5	5.7
0.45	100	8.5	7.2
0.27	120	4.7	4.8

When I_ℓ/B_z is large, there is a slight increase in the signal recorded with the larger electrodes. When I_ℓ/B_z is small, there is a decrease in signal with the wider electrodes. Any improvement in the total plasma trapped in the separatrix with the wider electrodes is only marginal.

(viii) Alteration of the gun current

The voltage V_g, to which the gun condenser bank was charged, was altered, keeping (a) the amount of gas in the plenum constant, and (b) N_p/V_g constant (where N_p = number of molecules in the plenum).

In both cases, the plasma signal recorded by the large ion probe was proportional to V_g. The ion probe signal had the same shape (approximately) as the gun current, so the amount of plasma trapped is presumably also proportional to the length of the gun current pulse. These two observations explain why the present gun is producing more trapped plasma than the original gun[1].

8. MEASUREMENT OF THE ENERGY OF THE PLASMA TRAPPED IN THE SEPARATRIX

8.1 Calorimetric Measurements

Copper foil, 0.0025 cm thick, was cut into the shape of the separatrix (as obtained from a computer program), and was suspended by thin wires, overlaying the separatrix. The temperature rise of the copper when the gun was fired was recorded with a calibrated copper-constantan thermocouple. The energy dumped by the plasma onto the copper could therefore be measured. The copper cooled slowly, making a cooling curve correction unnecessary.

The heat dumped onto the calorimeter is tabulated below, for different values of B_z and I_ℓ. The (estimated) total plasma energy contained in the separatrix is also recorded; recognizing that plasma produced by the gun travels both ways along the tube, approximately 67% of the plasma going one way and 33% the other, according to the direction of $B_{r\ell}$ at the gun.

B_z (tesla)	I_ℓ (kA)	Energy dumped by plasma on calorimeter	Energy of plasma contained in separatrix
		(± 10%)	(estimate)
0.09	40	1.18 J	1.77 J
0.18	80	2.34 J	3.5 J
0.27	120	3.1 J	4.65 J
0.36	160	3.64 J	5.46 J
0.45	200	3.8 J	5.7 J

An attempt was made to measure calorimetrically the heat carried by the escaping plasma to the vacuum tube walls; this was unsuccessful however, because of the excessive amount of heat dumped into the calorimeter by eddy-currents set up by the ℓ-winding current. Since approximately five times more plasma escapes than is trapped, the total energy of the escaping plasma is estimated as approximately 25 J when B_z is in the range 0.3 - 0.6 tesla.

The estimated total plasma energy (~30 J), plus the energy dumped into the gun electrode (~50 J) during the current pulse, does not amount to the total energy $\int I_{gun} V_{gun} dt$ fed into the gun by the condenser bank (~170 J). (Here, V_{gun} is the voltage maintained across the gun electrodes during the current pulse I_{gun}). The energy balance has not yet been accounted for.

8.2 Energy Analyzer Measurements (component of energy parallel to the magnetic field)

An energy analyzer similar in principle to the one used by Ashby et al[21] was used to measure the component of ion energy parallel to the magnetic field. Fig.22 shows the energy analyzer. The first grid repels

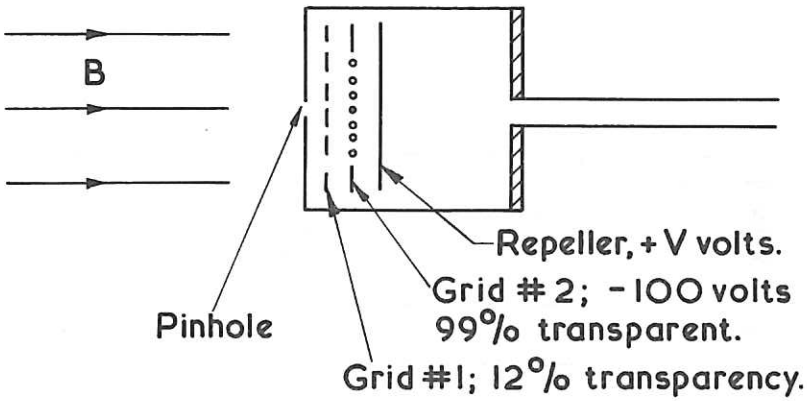

a

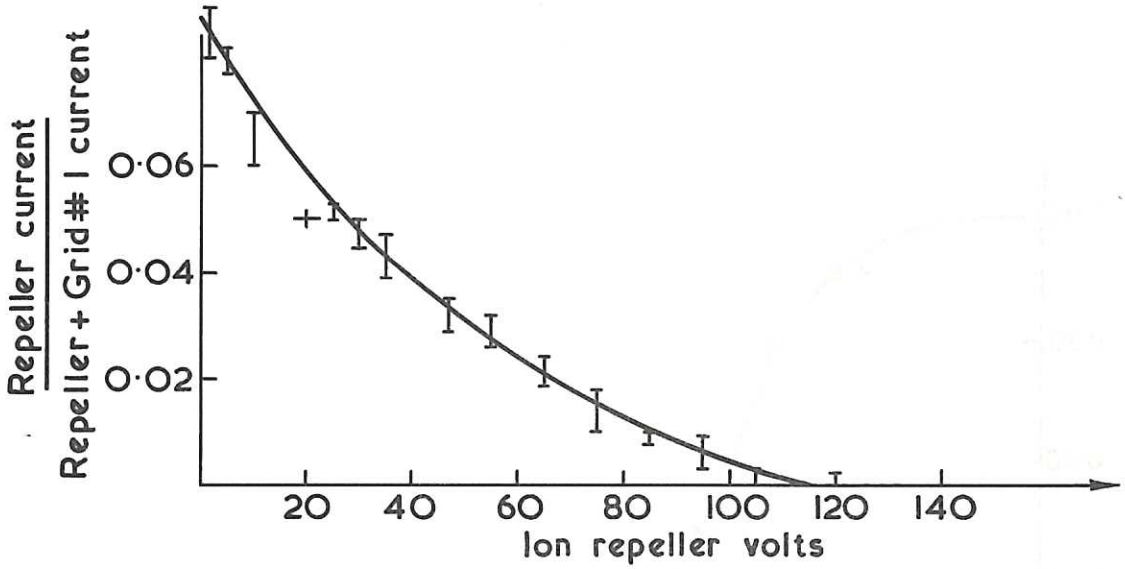

b

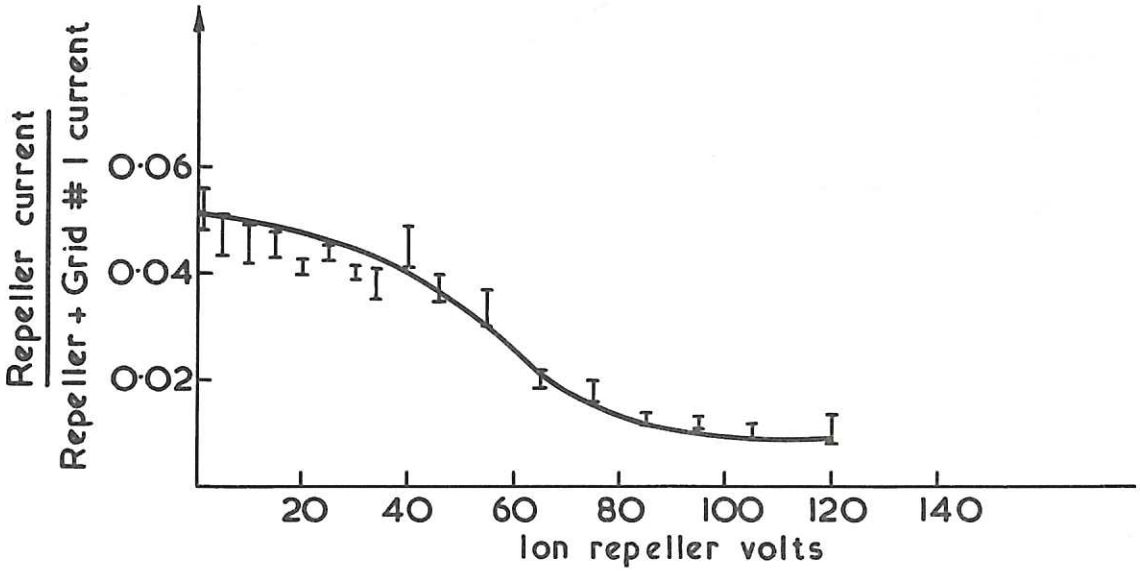

c

Fig.22 (a) The energy analyser.
(b) Results obtained with B_z = 0.36 Tesla, I_ℓ = + 160 kA.
(c) Results obtained with B_z = 0.36 Tesla, I_ℓ = - 160 kA.

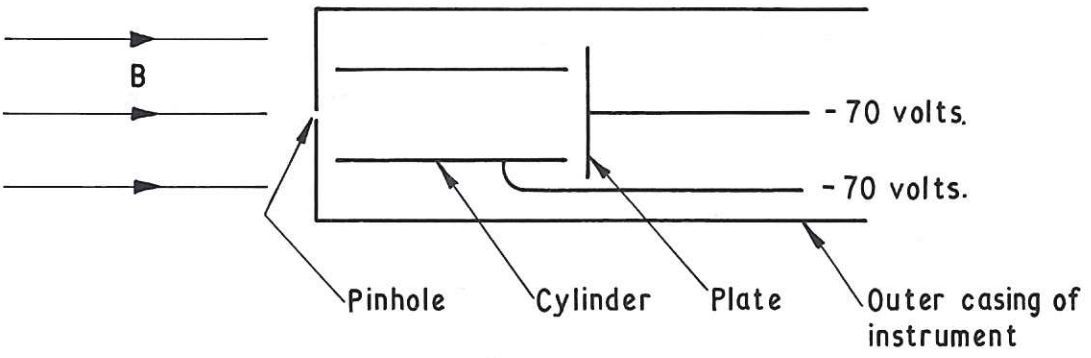

a

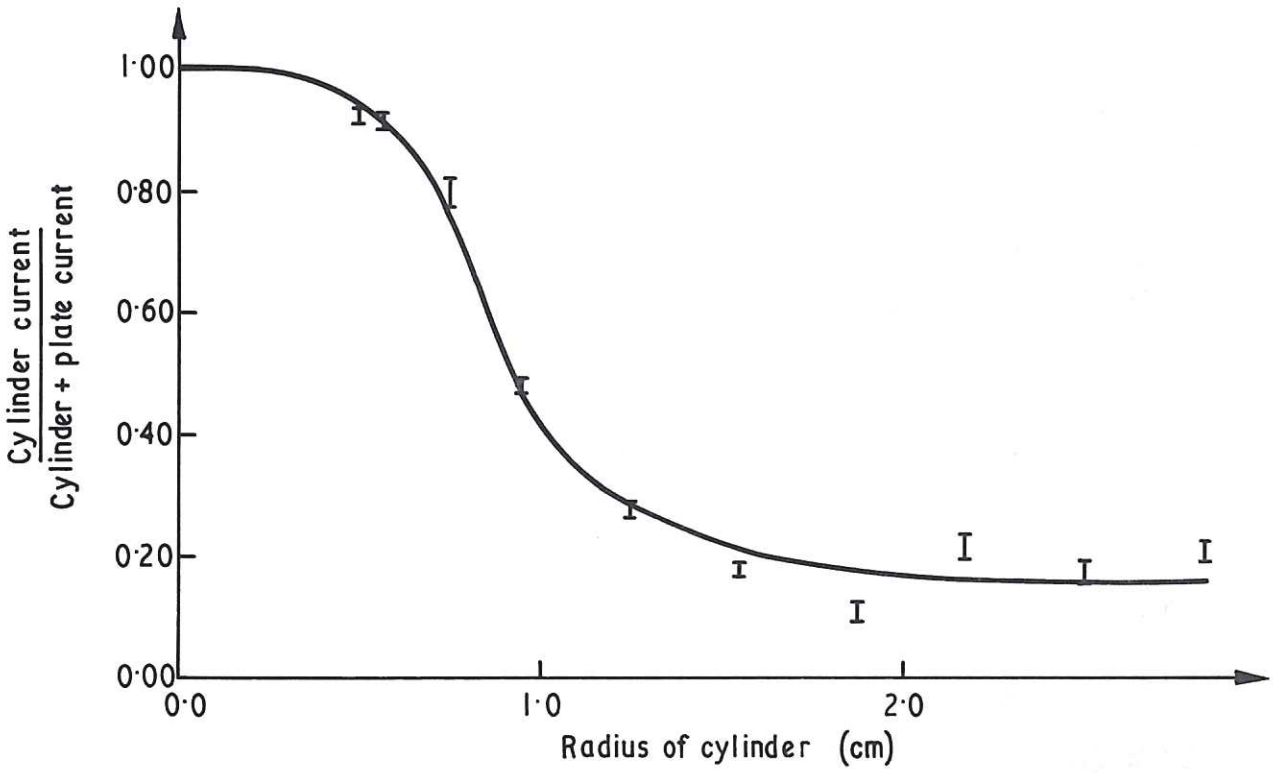

b

Fig.23 (a) Larmor radius analyser (b) Typical graph obtained with Larmor radius analyser. B_z = 0.36 Tesla, I_e = 0, d = 4.5 mm.

back to the outer casing of the instrument any electron approaching the grid. This grid is normally biassed to $-70\,V$, and has 12% optical transparency. The second grid is of 99% optical transparency and is biassed to $-100\,V$, and prevents any electron, produced on grid no.1 by secondary emission, from reaching the collector. The collector is biassed to a variable positive voltage $+V$. The ion current to the 1st grid and to the collector are both recorded on an oscilloscope. A plot of the ratio of collector current: grid # 1 current is also presented in Fig.22 for $B_z = 0.36$ tesla, $I_\ell = \pm\ 160$ kA. A mean ion energy along the magnetic field of 40 eV is indicated by the results for $+ve\ I_\ell$. With $-ve\ I_\ell$ the energy is ~ 60 eV.

Eubank[22] observed that the ion energy recorded by a similar energy analyzer may be too high by $\sim 3\,kT_e/e$ electron-volts, due to floating potential effects accelerating ions into the instrument. Since the electron temperature as measured with a Langmuir probe was in the range ~ 20 eV, the figure of 50 eV for the ion energy along the magnetic field must be regarded as an upper limit.

8.3 Measurement of the Component of Ion Energy Perpendicular to the Magnetic Field

The thermal energy of the ions transverse to the magnetic field was measured with a Larmor radius analyzer[1]. Measurements of this same thermal energy were also made by two new methods, but these results will be the subject of a separate paper[23]. The results of these two new methods agreed with the results obtained with the Ashby[1] type Larmor radius analyzer.

The instrument is shown in Fig.23. Ions from the plasma enter the pinhole of the instrument, which is aligned parallel to a uniform magnetic field. If the Larmor radius is greater than half of the radius of the cylinder, the ion will be collected by the cylinder. Otherwise, the ion will be collected by the plate. Fig.23 also shows the ratio of the plate current: total current to plate and cylinder, plotted against the diameter of the cylinder, with a gun electrode separation $d = 0.9$ cm.

The median Larmor radius and the median transverse ion energy are plotted against B in Fig.24, on the assumption that the plasma is hydrogen. It is seen that:

(a) The relationship $r_L \approx d$ holds in the regime $B \leq 0.3$ tesla, the regime studied by Ashby[1]. However, this relationship breaks down for larger values of magnetic fields, and $r_L < d$.

(b) The median transverse ion energy varies linearly with the applied magnetic field, and lies in the range 100 - 300 eV, depending

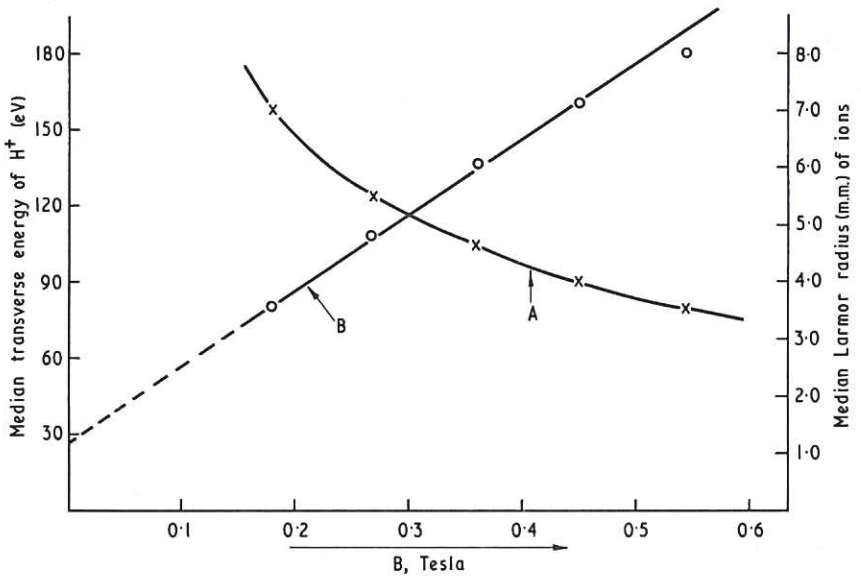

Fig.24 Median Larmor radius, and median transverse H^+ ion energy (on assumption that plasma is pure hydrogen plasma). The error of each point is ± 10% for curve A, and ± 20% for curve B.

upon the value of B. This is reminiscent of the result obtained by Bolton et al[6] for ion energy along magnetic field lines in a toroidal stellarator.

(c) About 20% of the ions of the plasma have a Larmor radius in excess of 15 mm. At $B_z = 0.4$ tesla, an H^+ ion with such a Larmor radius would have a kinetic energy in excess of 1800 eV. Such energies have not been detected with conventional energy analysers. It is probable that the large Larmor radius tail of Fig. 23 is the result of lower energy impurities of high atomic mass.

8.4 Langmuir Probe Measurements on the Trapped Plasma

A double Langmuir probe (of equal electrode areas) was inserted into the centre of the magnetic containment region at an axial distance z = 80 cm from the gun. The probe electrodes were each cylindrical of length 1.0 cm, diameter 0.1 cm, had a separation of 0.5 cm, and were placed at right-angles to the magnetic field.

The measurement was plotted point-by-point, the signal being recorded across a 100 Ohm resistance and integrated with a time-constant much longer than the gun current pulse. Fig.25 shows one Langmuir probe plot, typical of the several obtained under different conditions of B_z and I_ℓ. Under a wide range of B_z and I_ℓ, the temperature recorded by the Langmuir probe fell within the range 10-30 eV; however the results around 30 eV were difficult to analyze with certainty because the point at which saturation current occurs is not distinct here.

The number density of the plasma was measured by observing the ion current drawn by the probe at saturation[24] using:

$$I_+ = A_s \, ne \left(\frac{kT_+}{2\pi m_+}\right)^{\frac{1}{2}} ,$$

where A_s is the area of the sheath. This formula is appropriate in the regime of:

(a) $T_+ > T_e$ (ion temperature larger than electron temperature).

(b) Sheath thickness $d_s \ll r_p$, where r_p is the radius of the probe.

The magnetic field has little effect upon the saturation ion current drawn by the probe, since the ion Larmor radius is much larger than the probe radius.

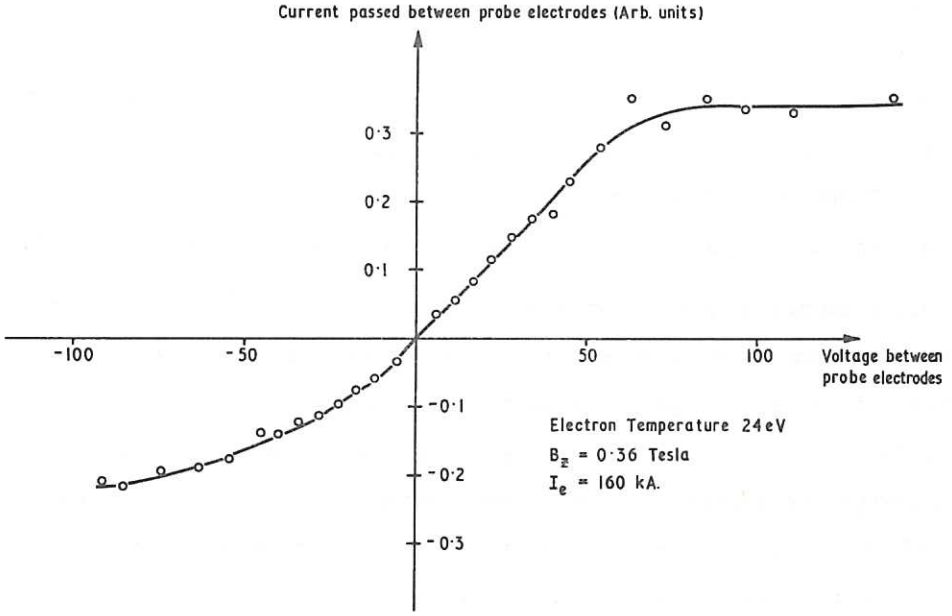

Fig.25 Double Langmuir probe plot. Each point is the average of three measurements.

Using the above formula and the value of ion temperature already obtained from the energy analyzer and the Larmor radius analyzer, the number density was measured to be:

$$n = 2.6 \times 10^{11} \text{ cm}^{-3} ,$$

at the time of maximum gun current, when $B_z = 0.36$ tesla , $I_\ell = 160$ kA .

An estimate of the number density can also be obtained from the large ion probe and the energy analyzer results. Let A_Δ be the area of the separatrix, and let I be the current drawn by the large ion probe, whose front screen has transparency α. Then :

$$n = \frac{I}{\alpha e}\left(\frac{m_p}{2E_\parallel}\right)^{\frac{1}{2}} \times \frac{1}{A_\Delta} .$$

The value of number density thus obtained agreed, within the experimental error, with the results obtained with the double Langmuir probe.

The time for equipartition of electron energies in a plasma, is given by Spitzer[25], and has been calculated to be $\sim 8.0\,\mu$sec for a plasma of number density 2.6×10^{11} cm^{-3} and temperature 20 eV. The plasma, which has a directed energy of 50 eV per H^+ ion along the magnetic field, will take $\sim 8.0\,\mu$sec to travel the 80 cm from the gun to the Langmuir probe. The equipartition of energy between the electrons will therefore be incomplete. Under such circumstances a double Langmuir probe measures the energy distribution of the electrons around the non-Maxwellian high energy tail of the distribution. Our Langmuir probe therefore measures an upper limit to the electron temperature.

8.5 Measurement of the Kinetic Energy of the Escaping Ions in the Component along the Magnetic Field

An energy analyzer similar to the one described earlier, was constructed. The only difference was that the front face of the analyzer, and its grids were at an angle to the main axis of the instrument, (Fig.26). The angle was such that, with the analyzer outside the separatrix at radial position $r = 12$ cm, the grids of the instrument could be aligned perpendicular to the local magnetic field, (as determined from a computer program).

Fig.27 shows a plot obtained with this instrument. Comparison of Figs.22 and 27 show that the energy of motion parallel to the local magnetic field is less in the escaping plasma than in the trapped plasma. This is believed to be the result of the changing $|B|$ along the escape line ABC of Fig.15. A computer program shows that, when $B_{zo} = 0.4$ tesla and $I_\ell = 160$ kA, the value of $|B|$ along the escape line ABC varies from a minimum value 0.386 tesla to a maximum value of 0.419 tesla (which occurs at the position of the energy analyzer). Putting $E_{\parallel 1} = 40$ eV and $E_{\perp 1} = 300$ eV as the energies of motion along and transverse to the magnetic field at the position of minimum $|B|$, one obtains from the conservation of energy and the adiabatic invariance of magnetic moment:

$$E_{\parallel 2} = \left(1 - \frac{B_{max}}{B_{min}}\right) E_{\perp 1} + E_{\parallel 1}$$

$$= 14 \text{ eV}$$

where $E_{\parallel 2}$ is the energy of ions parallel to $\underline{B}$ at the position of maximum $|B|$. This is in good agreement with the observed energy.

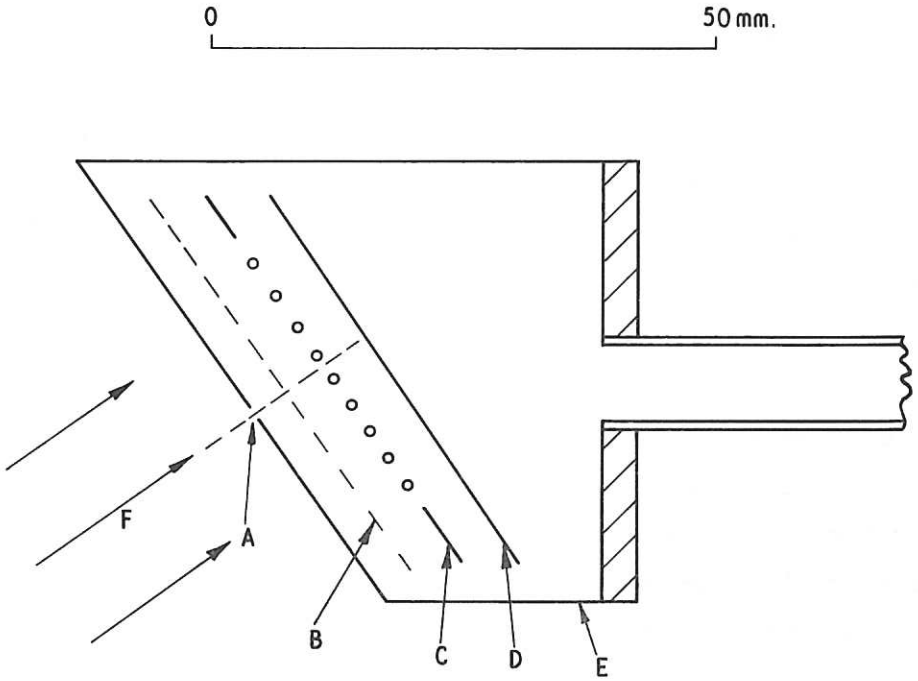

Fig.26 Energy analyser, for measuring the kinetic energy of the escaping ions, in the component along the local magnetic field. A: pinhole. B: grid 1, 12% transparent, biased to -70 V. C: grid 2 - 100 V, 99% transparent. D, ion repeller, biased to +V volts. E, outer casing of instrument. F is the local magnetic field.

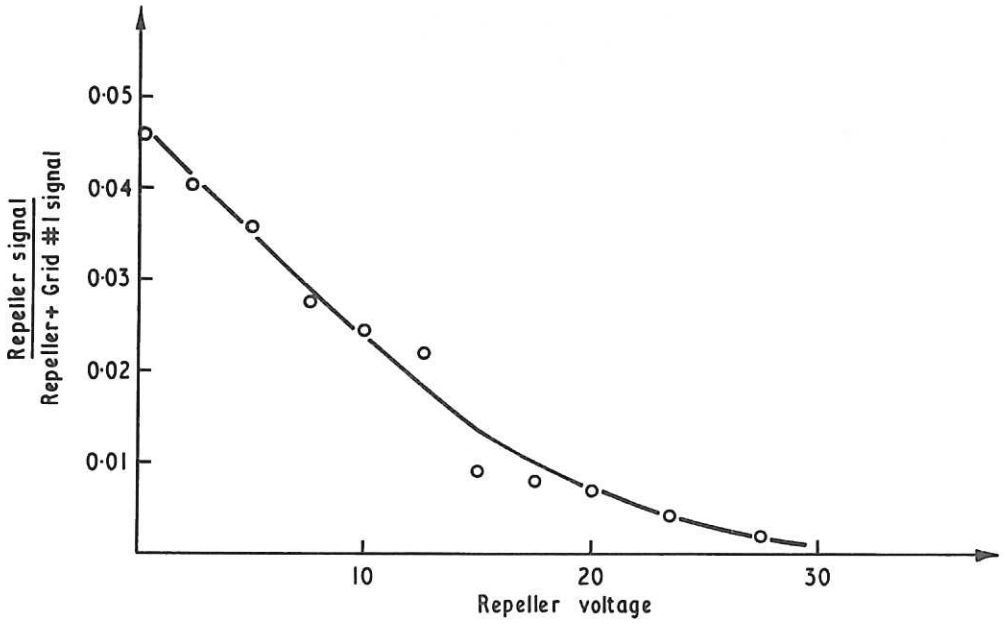

Fig.27 Results obtained with energy of escape analyser pointing along local magnetic field line, at position r = 0.12 metre, z = 0.23 metre, B = 0.36 Tesla, I_ℓ = 113 kA.

9. PREDICTION OF THE SUITABILITY OF THE PLASMA PRODUCED BY THE PRESENT INJECTOR FOR FILLING A TOROIDAL STELLARATOR

The present injector produces a plasma whose ions have a larger thermal energy transverse to the magnetic field than along the magnetic field. This injector will eventually be used to fill a toroidal stellarator. Gibson et al[20] considered a toroidal stellarator of major and minor radii R_o and r, containing p magnetic field periods. They showed that there are three types of particles that may appear in the toroidal stellarator, namely passing, blocked and localized particles. Let r_m = maximum radius of the separatrix. Then, for containment of all passing particles originating at radial position r_o:

$$\frac{1}{r_L} \geq \frac{48\, R_o^{\frac{1}{2}}\, r_m^2\, (r_m + r_o)^{\frac{1}{2}}}{p\left(r_m^4 - r_o^4\right)} \quad .$$

Suppose the present injector is used to fill a toroidal stellarator of major radius 0.9 metres, whose separatrix radius is 0.09 metres, and which has $p = 7$ field periods. The Larmor radius of the ions produced by the present accelerator had been measured to be ~ 0.003 metres. One obtains the result that the passing particles with $r_o < 0.05$ metres will be contained.

We now consider the containment of the localized particles produced by the present injector. The condition for localization, given by Gibson et al[20] is:

$$\frac{E_\parallel}{E_\perp} \leq \frac{\sqrt{2}}{27}\, \frac{p^2\, r_1^5}{R_o^2\, r_m^3} \, .$$

For an isotropic distribution of velocities, the fraction of the particles which are localized is[20]

$$f \approx \frac{p r_m}{12\, R_o}$$

$$= 7/120 \quad \text{for the parameters currently under consideration.}$$

For a plasma with energy $E_\parallel = 50$ eV and $E_\perp = 300$ eV, the fraction that are localized will be even higher. This is an undesirable feature of the present accelerator.

We now consider the expected Bohm containment time of a plasma injected into a toroidal stellarator by the present injector. The Bohm time is given by equation (4) as:

$$\tau_B = \frac{2.8\, B\, r_p^2}{T_e} \qquad \text{(M K S units).}$$

Suppose the plasma radius is ~ 0.09 metres, $B = 1$ tesla, $T_e = 30$ eV (corresponding to the upper limit of our electron temperature measurements) then:

τ_B = 0.76 ms.

An actual containment time of ~10 τ_B is expected, i.e., ~7.6 ms containment time.

Previous results [2,4,5,6] indicate that cross-field injection of plasma into toroidal stellarator magnetic fields is possible, even without the use of shorting plates. It is to be presumed that the plasma stream is depolarised by current flow along the rotationally transformed magnetic field lines of the magnetic trap. This mechanism is analagous to the better-documented case of plasma self-depolarisation in a toroidal octupole.[7]

10. CONCLUSIONS

The gun produces a plasma whose ions have kinetic energy transverse to the magnetic field of ~200 eV and along the magnetic field of ~50 eV. The electron temperature is about ~20 eV. Of the ~4 x 10^{17} electron ion pairs produced by the gun, only ~20% are trapped in the separatrix. A theory for the escape of a substantial portion of the plasma has been described.

The amount of plasma trapped in the separatrix is insensitive to changes of parameters such as separatrix size, magnetic field, distance of the gun from the separatrix, etc. The only parameters that have a pronounced effect in this respect are the gun current and the duration of the gun current. Because of electrode melting, there is little prospect of further increasing these parameters above the values used in this paper.

ACKNOWLEDGEMENTS

The author thanks the Manufacture & Installation, and the Engineering Design Groups of Culham Laboratory for constructing the apparatus.

This paper is a continuation of the work started by Mr. D E T F Ashby, whom the author wishes to thank for his help and advice during the early days of the experiment.

It was a particular pleasure to have worked with Mr. J. N. Burcham, who obtained many of the experimental results and made many useful suggestions.

REFERENCES

1. ASHBY, D. E. T. F., Plasma Physics 10, 665 (1968).
2. ASHBY, D. E. T. F. et al., Experiments on plasma injection heating and confinement in stellarators. 3rd Conference on Plasma Physics and Controlled Nuclear Fusion Research, Novosibirsk, USSR., August, 1968. Proceedings, Vol. 1. pp 573-590.
3. ELLIS, R. A. Jr. and EUBANK, H. P., Phys. Fluids 11, (5) 1109 (1968).
4. AKULINA, D. K. et al., Conference on Plasma Physics and Controlled Thermonuclear Fusion Research, Culham, England. September 1965. Proceedings, Vol. 2, pp.733-749. Culham Laboratory Translation CTO/232.
5. AKULINA, D. K. et al., Lebedev report (unnumbered) July 1966. Culham Laboratory Translation CTO/372.
6. BOLTON, R. et al., Phys. Fluids 14, (7) 1566 (1970).
7. DORY, R. A. et al., Phys. Fluids 9, (5) 997 (1966).
8. BARNEY, G. O., Phys. Fluids 12, (11) 2429 (1969).
9. BAKER, D. A. and HAMMEL, J. E., Phys. Fluids 8, (4) 713 (1965).
10. BAKER, D. A. and HAMMEL J. E., Phys. Rev. Letters 8, (4) 157 (1962).
11. BOSTICK, W. H., Phys. Rev. 104, (2) 292 (1956).
12. SCHMIDT, G., Phys. Fluids 3, (6) 961 (1960).
13. ZIKOV, V. G. et al., Plasma Phys. and Problems of Controlled Thermonuclear Fusion. Kiev 1965, pp. 27-36. Culham Laboratory Translation CTO/290.
14. ASHBY, D. E. T. F. (1968). Private communication.
15. VALSAMAKIS E. A., Rev. Sci. Instr. 37, (10) 1318 (1966).
16. COLE, H. C., Thesis, London University, January 1970.
17. NEDOSPASOV A. V. and SHIPUK, I. Ya., Teplofizika Vysokikh Temperatur 3, (2) 185 (1965). English translation in High Temperature (USSR) 3, (2) 166 (1965).
18. LINDBERG, L. and KRISTOFERSON, L., Royal Institute of Technology, Stockholm, Division of Plasma Physics, Report No. 69-16b, (1970).
19. SPROTT, J. C., Rev. Sci. Instr. 37, (7) 897 (1966).
20. GIBSON, A. and TAYLOR, J. B., Phys. Fluids 10, (12) 2653 (1967).
21. ASHBY, D. E. T. F. et al., AIAA Journal 3, 1140 (1965).
22. EUBANK H. P., (1965) Private communication to D. J. Lees, Culham Laboratory.
23. CHAMBERS, R. G., to be published.
24. SWIFT J. D. and SCHWAR, K. J. R., Electrical Probes for Plasma Diagnostics. Iliffe Books Ltd, (1970).
25. SPITZER L., Physics of Fully Ionised Gases, 2nd Ed. Interscience Publishers, (1962).

Available from

HER MAJESTY'S STATIONERY OFFICE

49 High Holborn, London, W.C.1
13a Castle Street, Edinburgh 2
109 St. Mary Street, Cardiff CF1 1JW
Brazennose Street, Manchester M60 8AS
50 Fairfax Street, Bristol BS1 3DE
258 Broad Street, Birmingham 1
7-11 Linenhall Street, Belfast BT2 8AY

or through any bookseller.